

JP

FINAL REPORT

MODEL DEVELOPMENT TO PREDICT
HYDROCARBON EMISSIONS FROM
CRUDE OIL STORAGE AND TREATMENT TANKS

James R. Beckman

Agreement No. A4-045-32

July 20, 1986

*1986
C-2*

FINAL REPORT

MODEL DEVELOPMENT TO PREDICT
HYDROCARBON EMISSIONS FROM CRUDE OIL
STORAGE AND TREATMENT TANKS

Abstract

A computerized mathematical model was developed to predict hydrocarbon emissions from crude oil storage and treatment tanks. The model predicts emissions from tanks that experience working, breathing and flashing effects. Tanks simulated include wash, lease automatic custody transfer (LACT) and shipping tanks. Sensitivity analysis of all model input variables on emissions was performed along with a comparison of two test cases selected by ARB from 1977 WOGA field test data. One test case involving working and breathing effects showed excellent agreement in hydrocarbon emissions and total off gas values. The other test case dominated by flashing effects showed excellent agreement in total hydrocarbon emissions, but it had 80% more predicted total off gas when compared with WOGA data and propane + emissions were low by 230%.

Acknowledgements

This work was performed in close association with Mr. John Courtis and Mr. Harry Metzger of the Industrial Section of the California Air Resources Board. Dr. Robert Grant, contract manager, assisted the research effort in maintaining a scheduling vigilance. The technical content of the progress reports was monitored by Mr. Robert Farnham of Innovative Analysis/Solutions who is contracted through WOGA. Mr. Farnham's comments significantly helped modify and direct the mathematical model development. Also inputs by representatives of EPA and industry helped form the scope of the project.

This report was submitted in fulfillment of A4-045-32 "Model Development to Predict Hydrocarbon Emissions from Crude Oil Storage and Treatment Tanks" by James R. Beckman under the sponsorship of the California Air Resources Board. Work was completed July 20, 1986.

Table of Contents

List of Figures.....	xi
List of Tables.....	xii
Summary and Conclusions.....	1
Introduction and Scope.....	3
Mathematical Model.....	6
Momentum.....	6
Species.....	12
Energy.....	17
Flashing.....	23
Model Simulations.....	26
Breathing Loss.....	26
Working Loss.....	36
Flashing Loss.....	37
Case Study A (Union 8826).....	42
Case Study B (Exxon 410).....	45
Central Processing Unit (CPU) Time Reduction Study.....	47
Computer Program Methodology.....	50
References.....	63
Glossary of Terms.....	65
Appendix (Program Listing).....	78

List of Figures

Figure 1 Cartesian Coordinates Approximating a Cylindrical..... 9
Boundary (top view)

Figure 2 Momentum Equation Boundary Conditions (Side View).....11

Figure 3 Species Equation Boundary Conditions (Top View).....13

Figure 4 Species Equation Boundary Conditions (Side View).....16

Figure 5 Energy Equation Boundary Conditions (Side View).....18

Figure 6 Temperatures and Vent Velocity versus Time in a28
Breathing Tank

Figure 7 Vent Velocity and Vent Hydrocarbon Concentration.....30
versus Time in a Breathing Tank

Figure 8 Example: Vent Port Location.....56

List of Tables

Table 1	Variables Affecting Breathing Loss.....	39
Table 2	Crude Liquid Composition.....	39
Table 3	Base Case 24 Hour Breathing Emissions.....	39
Table 4	Liquid Outage Effect on Emissions.....	40
Table 5	Gas Phase Diffusivity Effect on Emissions.....	40
Table 6	Working Loss Emissions.....	40
Table 7	Flashing Loss Emissions.....	41
Table 8	Case Study A (UNION 8826) Predicted Emissions.....	44
Table 9	Case Study B (EXXON 410) Predicted Emissions.....	46
Table 10	Central Processing Unit (CPU) Time Reduction Using a..... Basis 4 Cycles (95% Terminal State Emissions) Starting at 3:00 a.m.	49
Table 11	Central Processing Unit (CPU) Time Reduction Using..... 3:00 p.m. Starting Time	49
Table 12	Program Assumed Vapor/Liquid Equilibrium K Values.....	54

Summary and Conclusions

A mathematical model was developed to predict hydrocarbon emissions from crude oil storage and treatment tanks. The model predicts emissions from crude oil wash, lease automatic custody transfer (LACT), and shipping tanks. Tank emissions are affected by combinations of working, breathing, and flashing effects. Working effects on emissions result from liquids being pumped into or out of a tank liquid basin. Breathing effects on emissions result from the solar heating and cooling of the tank gas space. Flashing effects on emissions result from the gas generation by pressure release of hot high pressure crude feeds. Because of the complexity of the model, a computer program was required for solution. Ultimately, tank field tests will be required by ARB to verify the accuracy of model predicted emissions.

Field crude oil tanks maybe a significant source of hydrocarbon emissions which depend solely on flashing, working, and breathing effects. Previous to this study accurate prediction methods did not exist but were needed to accurately determine the magnitude of hydrocarbon emissions to help assess the level of cost-effective emission controls.

In order to establish a model for emissons from crude oil tanks the project was structured into two phases; Phase I consisted of meeting with ARB, EPA, WOGA, and industrial personnel to discuss and complete a list of major process variables and to agree on differential equations and boundary conditions that were pertinent to the problem. Phase II consisted of developing a computer program that solved the equations from Phase I, testing the major variables for sensitivity to emissions, and simplifying the complex model as much as possible together with user friendly input formating for industrial and government end users.

The model focused attention on the gas space inside the tank. In the gas space fluid momentum, hydrocarbon species and energy partial differential equations were solved simultaneously. Solar effects were included in simulating as closely as possible environmental effects on establishing tank wall and dome metal temperatures.

Model input variable sensitivity on predicted hydrocarbon emissions were examined by both a single phenomenon and a case study approach. The single phenomenon simulations involved only one of the emitting mechanisms (i.e., working, breathing or flashing effects). The simulations used large variable movements to identify the largest reasonable effects on emissions. The case study approach analyzed the effect of model input variables on two field tanks tested by WOGA and selected by ARB in which all three emitting mechanisms were simultaneously involved. Some of the input data for these cases had to be estimated, since they were not included in the WOGA report. The case studies used variable movements on the order of data error to judge the sensitivity to predicted emissions.

In the single phenomenon study when solar breathing was selected as the only emitting function, the major variables that affected emissions were tank diameter, liquid phase composition, and vapor/liquid equilibrium constant values. When flashing effects on emissions were investigated from a water/hydrocarbon feed stock, liquid feed temperature was found to be the most important variable in determining both total off gas and hydrocarbon emissions. Working loss emissions were dominated by the magnitude of the change of liquid volume.

In the case study analysis two tanks from the 1977 WOGA field test were selected by ARB for comparison. Tank "A" was UNION oil tank 8826 which was experiencing working and solar breathing effects. The model predicted

emissions were 22 lb/day total hydrocarbon of which 6 lb/day was methane plus ethane. WOGA data showed 21 lbs/day total hydrocarbon with 1.5 lb/day methane plus ethane. Total emitted gas volume was predicted at 530 cu ft/day compared with the data value of 595 cu ft/day.

Tank "B" was EXXON 410 which involved flashing crude/water feed stock from 35 psig 170°F to atmospheric conditions along with liquid surface working. Analysis showed that the amount of flashed vapor volume dominated working effects so the tank never inhaled ambient gas. The model predicted total emissions of 1560 lbs/day containing 1270 lb/day methane and ethane. WOGA data listed 1518 lb/day total emissions with 555 lb/day of methane and ethane content. In both tank "A" and "B" cases the methane/ethane portion of emissions was predicted to be about three times larger than the data values. In order for the model to agree with the WOGA data, the vapor/liquid equilibrium constants must be reduced for methane/ethane and increased for propane through decane. However, there are no data to justify such a reassignment of values.

Introduction and Scope

Some field crude oil production and storage tanks may be significant sources of hydrocarbon emissions; these emissions may vary as a result of flashing, working, and standing effects. Prediction methods were needed to determine as accurately as possible the amount of hydrocarbon emissions and to help assess the level of cost-effective emission controls. Available predicting methods determined breathing and working losses from tanks containing stabilized crude oil and products but were not applicable to exact working, breathing, and flashing conditions experienced by a tank under study. The objective of this project was to develop mathematical

models that would consider all major variables, to predict emissions from wash, lease automatic custody transfer (LACT), and shipping tanks which were experiencing working, breathing, and flashing effects.

Available predicting methods were developed by the American Petroleum Institute (1957, 1959, 1962) to determine breathing and working losses from tanks in general but were not applicable to exact working, breathing, and flashing conditions experienced by a tank under field study. Beckman (1983, 1984), Beckman and Gilmer (1981), and Beckman and Holcomb (1986), have modeled breathing and working losses for idealized tanks, but their techniques were not applicable to tanks experiencing asymmetrical conditions and certainly not applicable to cases involving a flashing phenomenon.

Working losses of gasoline and crude oil storage have been investigated by the American Petroleum Institute (API) (1962). Their predicting equation was empirical and was based on emissions from 123 tanks. However, the correlation was generated for some undefined general operating condition. Beckman (1983), Beckman and Holcomb (1986), and Holcomb (1983), presented a model of working loss emissions at terminal state by a liquid surface being worked by a sawtooth wave. The model assumed gas phase plug flow in which hydrocarbon from the liquid surface diffused upward through the gas strata to reach the top dome vent and emit to the atmosphere.

Standing loss emissions from storage tanks have also been investigated by the API (1957, 1959, 1962). The resulting empirical equation was based on data from 64 tanks containing gasoline and 15 tanks containing crude oil. The model was modified by EPA (1981) by a factor of 0.6 after the 1977 WOGA study (Engr-Sci, 1977), since the previous model overpredicted measured emissions from 21 industrial storage tanks. Beckman and Gilmer (1982) improved the prediction of hydrocarbon breathing losses by posing a gas

phase mass diffusion controlled model for hydrocarbon movement inside a storage tank. Their analysis was successful in predicting breathing emissions to within 30% for the three cases considered. Beckman (1984) suggested a simultaneous heat and mass transfer diffusion model in which the temperature of the top dome was sinusoidal between temperature limits established by solar radiation on the dome. Predicted breathing emissions agreed closely with the emission data from 6 industrial tanks involved in the 1977 WOGA tests (Engr-Sci, 1977). Gustria (1983) and Sahakian (1983) also pursued breathing emission effects on a laboratory based tank and found significant radiation effects internal to the tank gas space.

In order to establish a mathematical model which would predict working, breathing, and flashing emissions from an exact field tested crude storage tank, the project was structured into two phases by ARB (memo to J. R. Beckman from F. DiGenova, September 26, 1984).

Phase II was accomplished by six progress reports covering "Tank Gas Phase Velocity" (No. 1 September 13, 1985), "Working Loss Emissions" (No. 2 October 15, 1985), "Flashing Loss Effects" (No. 3 November 15, 1985), "Standing Loss Emissions" (No. 4 December 20, 1985), "Variable Sensitivity" (No. 5 March 7, 1986), and "Model Reduction with CARB Formatting" (No. 6 July 2, 1986). The progress and technical content of these reports were monitored by Mr. Robert Farnham of Innovative Analysis/Solutions who is contracted with Western Oil and Gas Association (WOGA). Mr. Farnham's comments significantly helped modify and direct the mathematical model development.

This study represented an important step toward attaining the capability to predict hydrocarbon emissions from tanks used to process and store crude oil. Such capability is urgently needed for development and

determination of the need for hydrocarbon control strategies for oil field tanks in the South Coast and San Joaquin Valley Air Basins.

The statements and conclusions in this report are those of the Contractor and not necessarily those of the State Air Resources Board. The mention of commercial products, their source, or their use in connection with material reported herein is not to be construed as an actual or implied endorsement of such products.

Mathematical Model

Momentum

It was proposed that one aggressive detailed model be developed to predict hydrocarbon emissions from fixed-roof storage tanks. The model included the effects of liquid surface working, crude feed flashing, and solar heating (breathing) on hydrocarbon emissions from a tank top vent into the atmosphere. In order to do this the model simultaneously solved the momentum, continuity, species, and energy equations.

The gas phase momentum equations, as given by Bird, Steward and Lightfoot (1960), for a cylindrical tank geometry were modified in several ways for this model. Firstly, the foundation paper of fluid flow from a basin into a pipe by Vretas and Duda (1973) showed that pressure gradients were insignificant compared to inertial and viscous terms in a fluid basin and can be deleted from the momentum Equations (1), (2) and (3). This results from the fact that the length of the vertical gas flow path is on the order of the horizontal flow path length, which is totally unlike the flow in a long pipe where pressure drop is highly significant. However, gas density generated pressure gradients have been kept in the vertical momentum

Equation (3) so that effects of both temperature and composition in the gas phase density on gas phase velocities was taken into account.

Secondly, due to the relatively low horizontal gas velocities experienced in crude fixed-roof storage tanks, the viscous terms dominated inertial effects, thereby allowing the inertial terms to be deleted from the horizontal momentum Equations (1), (2). Typically, liquid phase movement of perhaps 1.0 ft/hr will generate vertical gas velocities of 1.0 ft/hr to 5.0 ft/hr in the bulk of the gas phase and increase to 0.1 ft/sec in the top dome vent area. Maximum liquid phase velocities might be experienced during a rapid depletion of the liquid from a shipping tank. If a 20.0 foot high shipping tank were to empty in 2 hours, then the maximum vertical gas phase velocity would be about 1.0 ft/sec in the vicinity of the vent, and the bulk gas would experience a velocity of about 10.0 ft/hr. Even though vertical gas velocities are low, the vertical inertial term was kept in Equation (3), but inertial terms were deleted in the horizontal momentum Equations (1) and (2) to enhance computational speed.

Thirdly, because of the rapid response of gas phase velocity changes over compositional and thermal changes, a gas phase momentum pseudo-steady state assumption was made. This assumption deleted the time derivatives from the momentum equations and eliminated the necessity for storing past time gas velocity information, resulting in needed gas phase velocity computer storage being cut in half.

Fourthly, the continuity equation was introduced into the horizontal momentum Equations (2), (3) to improve material balance constraints (after the work of Browne (1978)).

Lastly, the coordinate system was changed from curvilinear to Cartesian to reduce the computational effort required by the program. The momentum

equations written in curvilinear coordinates are extremely coefficient intensive; whereas, in Cartesian coordinates the coefficients are essentially unity. The coordinate transfer resulted in a reduction in the computational effort by a factor of at least 3.5.

All of these modifications of the momentum equations led to the following usable forms:

Horizontal X Directional Momentum Equation

$$\frac{\partial^2 v_y}{\partial x \partial y} + \frac{\partial^2 v_z}{\partial x \partial z} = \frac{\partial^2 v_x}{\partial y^2} + \frac{\partial^2 v_x}{\partial z^2} \quad (1)$$

Horizontal Y Directional Momentum Equation

$$\frac{\partial^2 v_x}{\partial y \partial x} + \frac{\partial^2 v_z}{\partial y \partial z} = \frac{\partial^2 v_y}{\partial x^2} + \frac{\partial^2 v_y}{\partial z^2} \quad (2)$$

Vertical Z Directional Momentum Equation

$$(\rho - \bar{\rho})g + \rho v_z \frac{\partial v_z}{\partial z} = \mu \left[\frac{\partial^2 v_z}{\partial x^2} + \frac{\partial^2 v_z}{\partial y^2} + \frac{\partial^2 v_z}{\partial z^2} \right] \quad (3)$$

The above three gas phase momentum equations were solved simultaneously together with a horizontal planar adjustment check. This check was the integration of vertical velocity on any horizontal plane to assure mass balance in the vertical direction.

Planar Continuity Equation

$$I = \iint V_z dx dy \quad (4)$$

Adjustments in the vertical gas velocity using Equation (4) were minor, on the order of 1.0 to 10. percent.

Figure 1 is a top view of a cylinder as viewed with a cartesian grid. The computer program selects points on the grid closest to the circular boundary to closely simulate a circular figure. Grid points lying outside the circular figure are not used, and thereby, represent an approximate loss

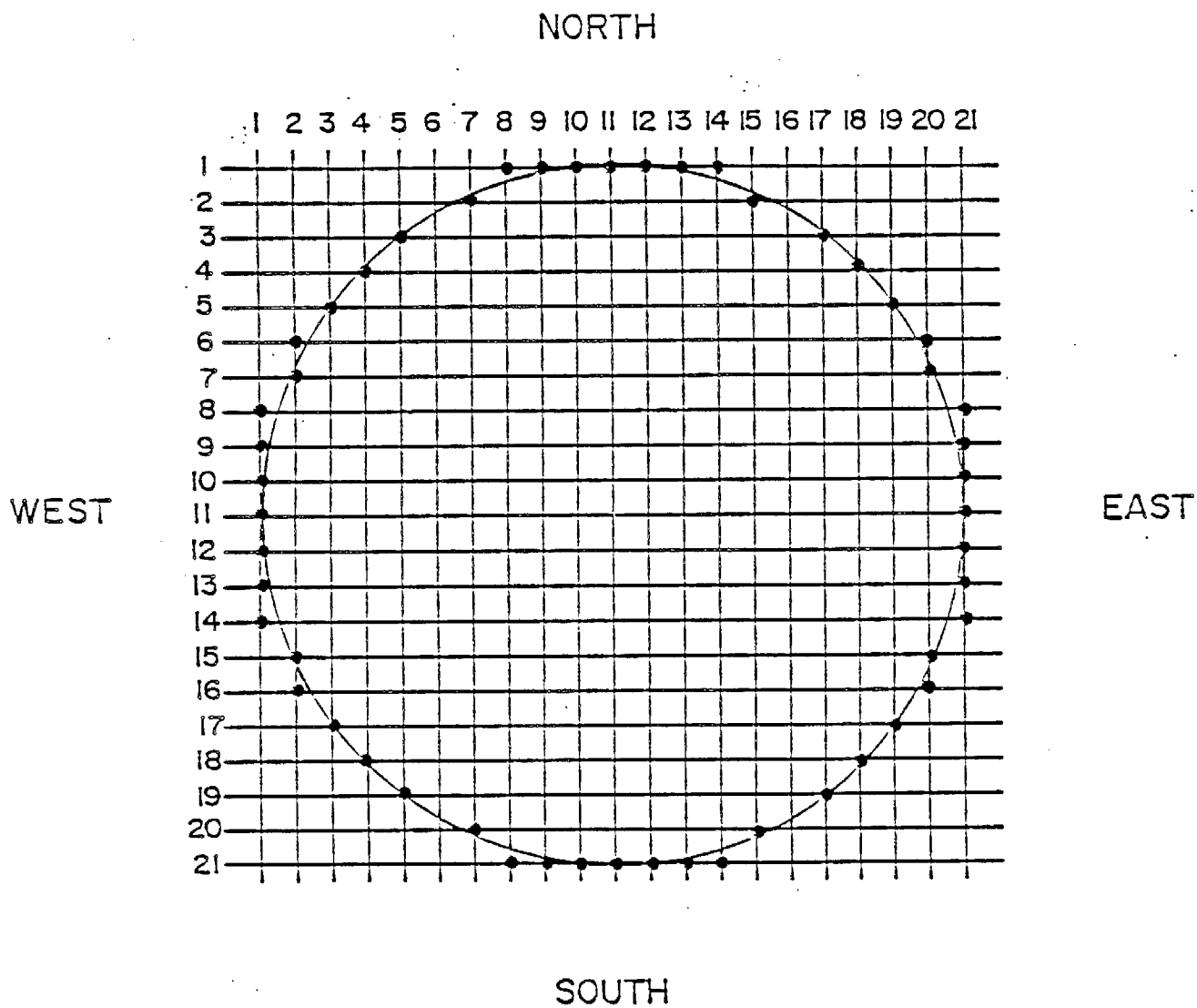


FIGURE 1
 Cartesian Coordinates Approximating a
 Cylindrical Boundary (Top View)

of 25 percent of the computer stored velocity matrix; however, the increase in computational speed by a factor of 3.5 more than offsets this disadvantage in computer storage.

Figure 2 is a tank side view showing the gas space velocity values at the walls, dome, and liquid surface.

The numerical technique used to solve equations 1, 2, and 3 was similar to the methodology used by previously successful investigators such as Vrentas and Duda (1973). Essentially the technique required central differencing of the spacial derivatives which gave a stable balanced approximation of the velocities. The momentum equations were solved for velocity using the Gauss-Seidel iterative method, and the solution methodology was stable since the equations possessed diagonal dominance.

The solution method was found to be stable and was quickly attained by starting the solution at the top dome plane and sequentially moving down to the liquid surface. At any plane, k , the vertical velocity, V_z , was solved by first using Equation (3). The value of V_z on the $k+1$ plane had to be assumed the same as the value on the k plane in order to calculate V_z on the $k + 1$ plane. This approximation was made for the first pass only in order to get the solution started. Subsequent calculations of V_z used the previous pass value of V_z on the plane to get updated values of V_z on the k plane. Results showed this technique to be extremely useful because only two passes down the tank gas space were needed for a converged solution. After V_z was calculated on a plane, the mass balance integral, Equation (4), was used to insure mass balance in the vertical direction. If mass balance was not achieved, the vertical gas velocities were adjusted. In all cases considered, this adjustment was between 1.0 and 10.0 percent of the mass balance integral, I . The horizontal velocities, V_x and V_y , were then

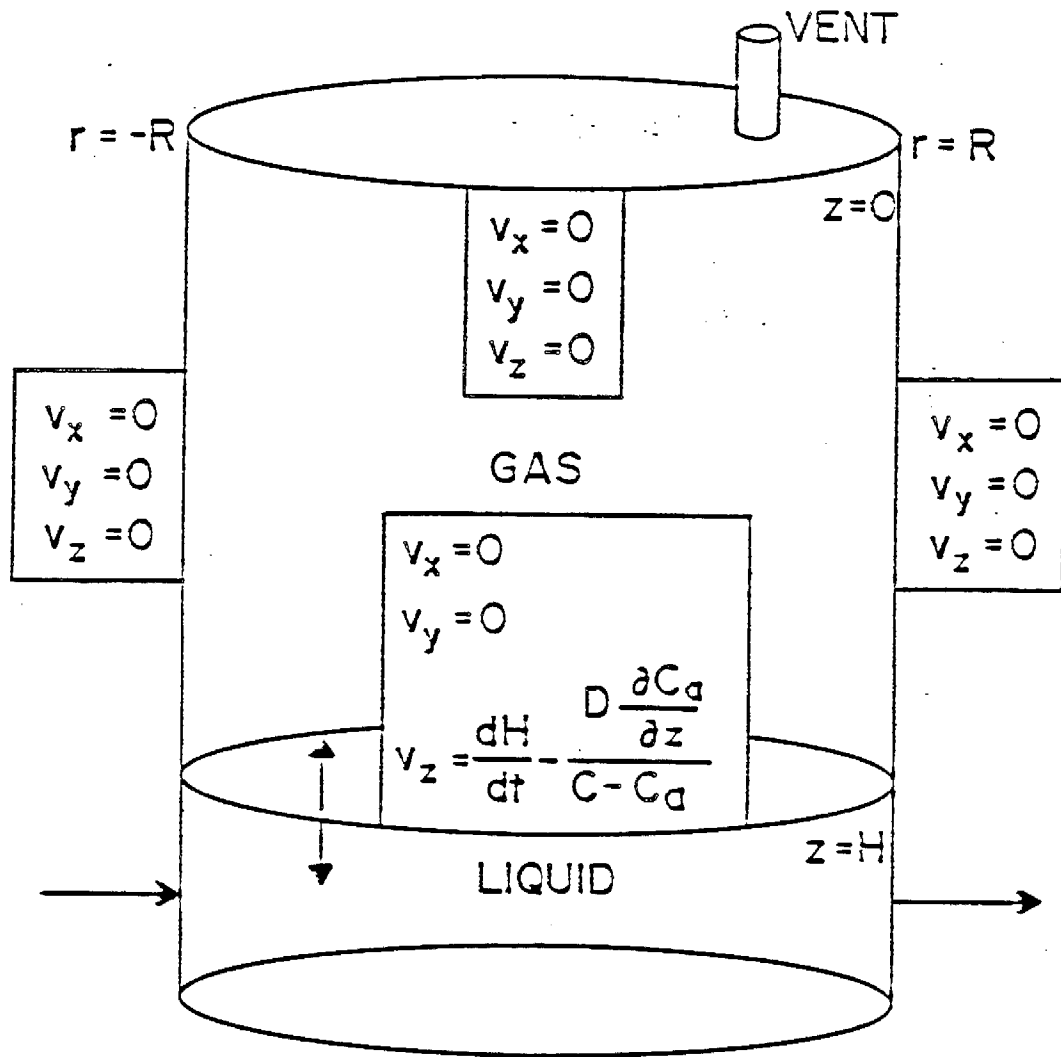


FIGURE 2

Momentum Equation
Boundary Conditions

calculated using Equations (1) and (2). After V_x , V_y , and V_z values had been calculated on a plane, the next lower plane was selected and the procedure repeated. At the liquid surface plane, the calculations were repeated starting at the top dome and sequentially moving down again to the liquid surface. In the cases considered, the values of the velocities remained within 1.0 percent of their previous pass estimates.

Species

The partial differential equation which describes the diffusion and bulk velocity transport of a chemical species within the gas space of a fixed-roof storage tank is given as Equation (5) (see Bird, Steward, Lightfoot ch.18).

$$\text{Dim} \left[\frac{\partial^2 C_i}{\partial x^2} + \frac{\partial^2 C_i}{\partial y^2} + \frac{\partial^2 C_i}{\partial z^2} \right] = \frac{\partial C_i}{\partial t} + v_x \frac{\partial C_i}{\partial x} + v_y \frac{\partial C_i}{\partial y} + v_z \frac{\partial C_i}{\partial z} \quad (5)$$

Equation (5) is written in Cartesian coordinates instead of curvilinear form in order to take advantage of reduced computational effort. Equation (5) was made discreet using central difference for the second order derivatives and forward difference for the time and inertial derivatives. These differences yielded excellent numerical stability.

The boundary condition at the side walls resulted from a zero mass flux and zero gas velocity constraint at the wall giving Equation (6):

$$y \frac{\partial C_i}{\partial x} + x \frac{\partial C_i}{\partial y} = 0 \quad (6)$$

By observing Figure 3 it can be seen that Equation (6) gives $\partial C_i / \partial y = 0$ at the left and right hand boundaries and $\partial C_i / \partial x = 0$ at the top and bottom boundaries. At the boundary positions located in between those mentioned, Equation (6) shows that there is a relationship between the concentration derivatives for all x and y values which is taken into account in the computer program.

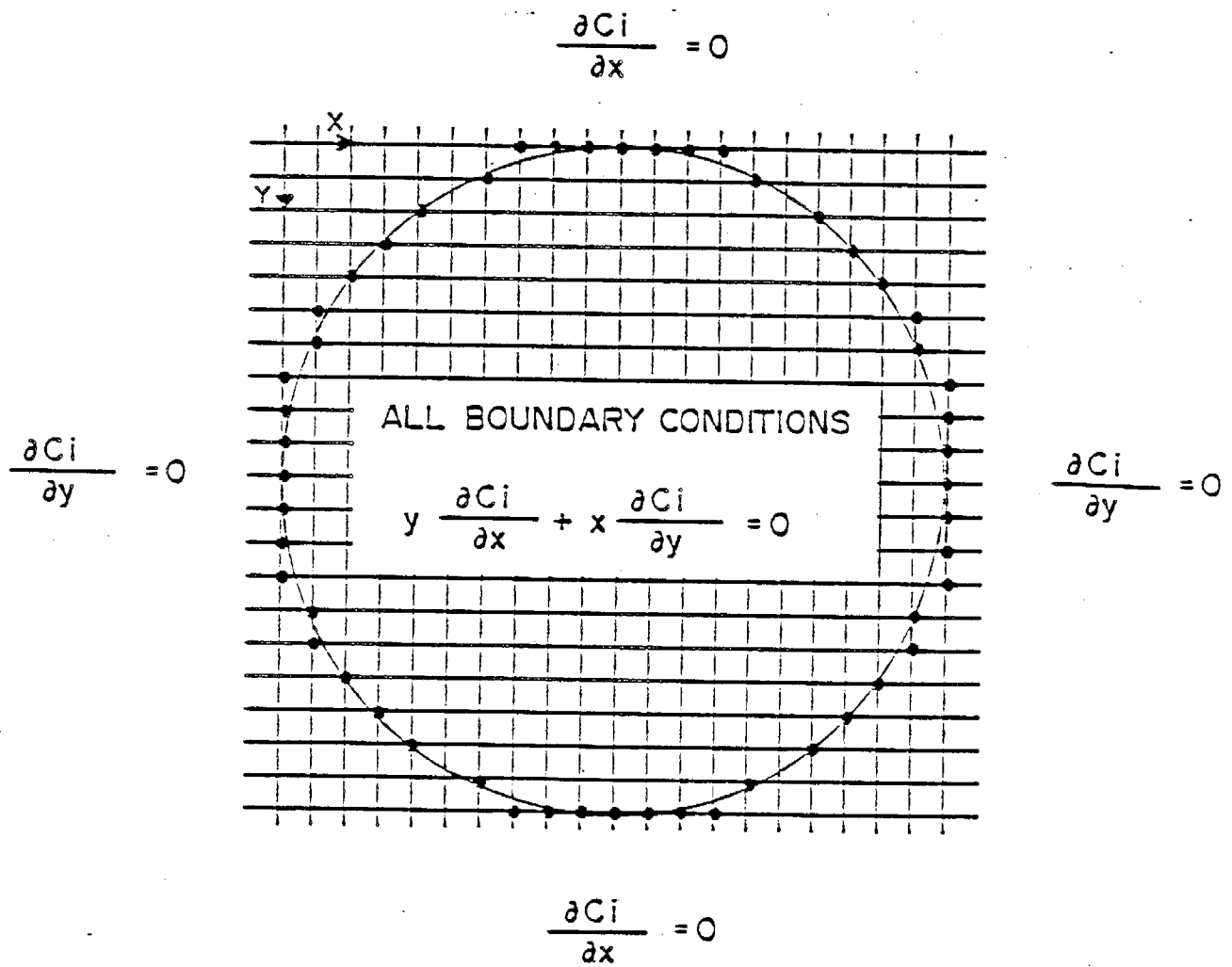


FIGURE 3

Species Equation Boundary Condition
Top View

At the top dome the concentration gradient with respect to the vertical direction is zero ($\partial C_i / \partial z = 0$). This condition is valid during exhale but not during inhale conditions at the vent ports which are located in the top dome. In the vent ports during gas inhale, the flux of all volatile species is considered to be zero, giving:

$$\frac{\partial C_i}{\partial z} (z = 0) = C_i v_z / \text{Dim} \quad (7)$$

Emission of each species is calculated by integrating the boundary concentration at the vent with respect to time to give the total amount of volatile species emitted, E_i .

$$E_i = \int C_i (\text{vent}) v_z (\text{vent}) dt \quad (8)$$

At the liquid surface the gas phase concentration, $C_i(\text{gas sur})$, is assumed to be in equilibrium with the liquid surface concentration, $C_i(\text{liq sur})$. These gas phase and liquid phase concentrations are related through the vapor/liquid equilibrium constant, K ;

$$C_i (\text{gas sur}) = C_i (\text{liq sur}) * K * C (\text{gas}) / C_{\text{liq}} \quad (9)$$

The value of K for each hydrocarbon is obtained from the DePriester charts (DePriester 1953) but could also be obtained from work currently being done at UC Davis (memo Holmes to Beckman 5/28/85). The value of K for a dissolved gas such as nitrogen, hydrogen, hydrogen sulfide and carbon dioxide were obtained from Edmister and Lee 1983 or could be estimated from experimental data.

The liquid phase composition at the liquid surface, $C_i(\text{liq sur})$, was related to the bulk liquid phase composition deep below the liquid surface, $C_i(\text{liq blk})$, by specifying a boundary layer film thickness, FILM , that a species would have to diffuse through. This assumption related the gas phase flux at the liquid surface, N_i (at $z=H$), to the bulk liquid

composition which allowed the depletion of volatile components at the liquid surface.

$$C_i (\text{liq sur}) = C_i (\text{liq blk}) - N_i (\text{at } z=H) * \text{FILM} / D_{il} \quad (10)$$

This type of boundary condition was needed in order to take into account the mixedness of the liquid phase. A small value of FILM such as 0.0001 ft would imply a well mixed liquid in which $C_i (\text{liq sur}) = C_i (\text{liq blk})$, whereas a large value of FILM would relate to a stagnant liquid phase where $C_i (\text{liq sur})$ could be much less than $C_i (\text{liq blk})$. A large value of FILM would be on the order of 1.0 feet. The variable, D_{il} , is the liquid phase diffusivity of a species. The value of D_{il} in Equation (11) was estimated by the Wilke correlation (Bird, Stewart and Lightfoot, Ch-16, 1960).

$$D_{il} = 7.4 * E^{-8} * (M_b^{.5}) * T * (C_i (\text{liq boil})^{.6}) / \mu \quad (11)$$

In Equation (11) M_b is the molecular weight of the mixture, T is the liquid temperature, μ is the liquid viscosity and $C_i (\text{liq boil})$ is the molar concentration of species "i" as liquid at its normal boiling point. Other values of D_{il} could be supplied to the program by the user.

The gas phase velocity in the vertical direction at the liquid surface is represented by Equation (12):

$$V_z (\text{at } z=H) = dH/dt + \sum N_i (\text{at } z=H) / C(\text{gas}) \quad (12)$$

Equation (12) is composed of two effects which establish the gas phase velocity at the liquid surface; 1) the velocity of the physically moving surface, dH/dt , and 2) the velocity resulting from all the species trying to evaporate into the gas phase. Together these two effects establish the effective velocity of the liquid surface.

Figure 4 is a tank side view showing the composition boundary conditions at tank internal surfaces.

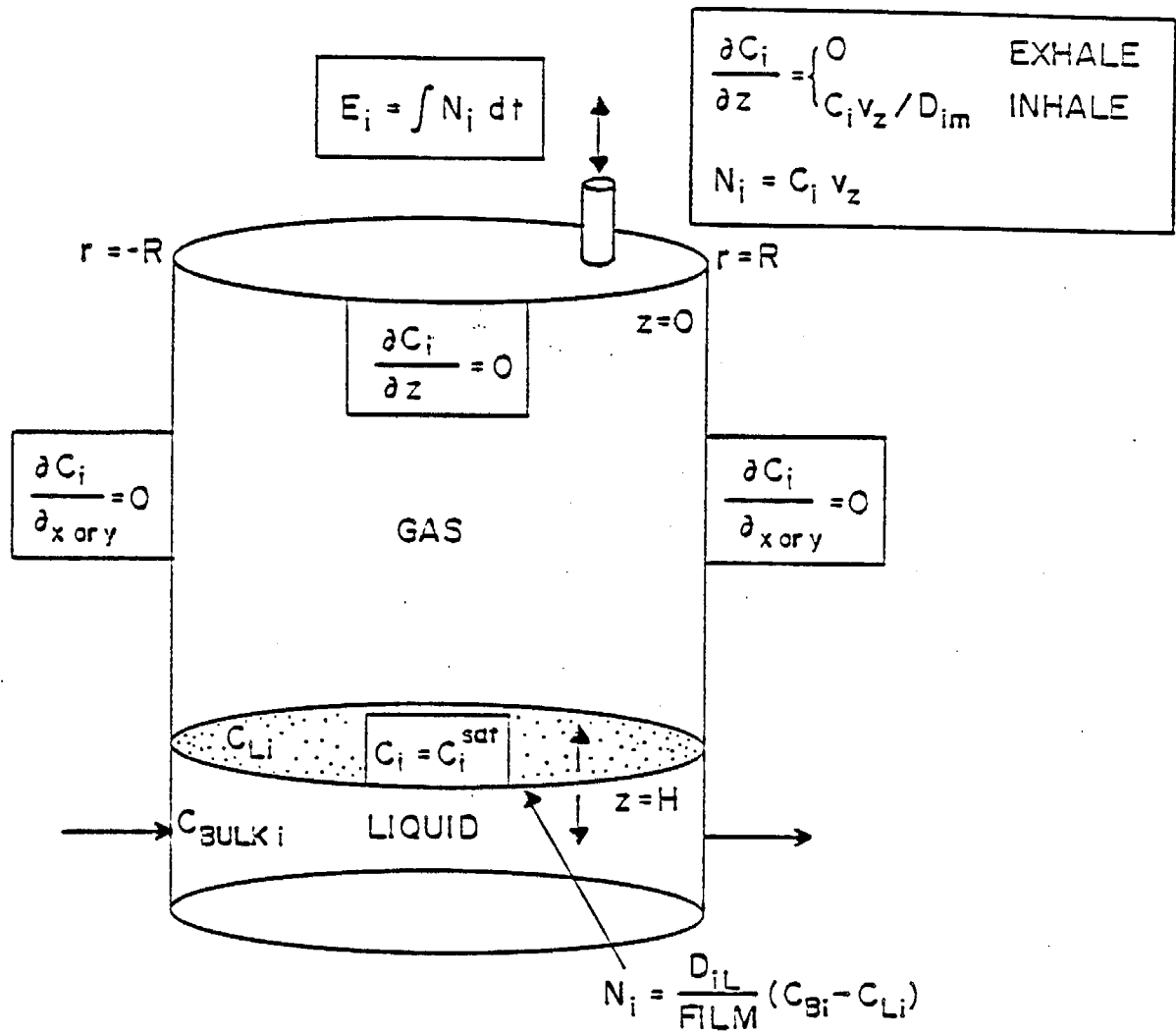


FIGURE 4

Species Equation
Boundary Conditions

Energy

The partial differential equation which describes the conduction and bulk velocity transport of energy (gas temperature) within the gas space of a tank is given by Equation (13) (see Bird, Stewart, Lightfoot, Ch-10 1960):

$$k \left[\frac{\partial^2 T}{\partial x^2} + \frac{\partial^2 T}{\partial y^2} + \frac{\partial^2 T}{\partial z^2} \right] = \rho \left[\frac{\partial T}{\partial t} + v_x \frac{\partial T}{\partial x} + v_y \frac{\partial T}{\partial y} + v_z \frac{\partial T}{\partial z} \right] \quad (13)$$

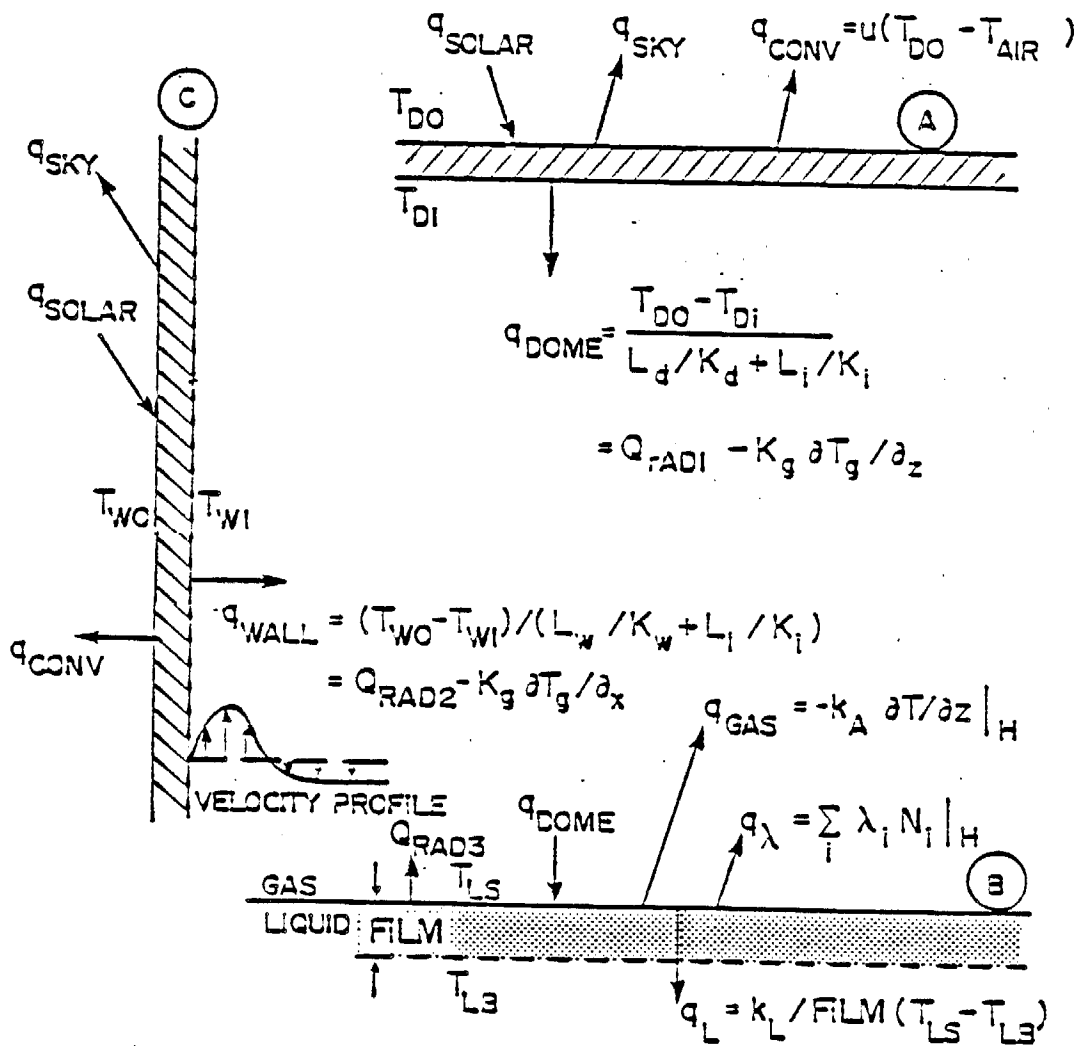
Equation (13) was discretized and numerically solved in the same manner as the species equation (Equation (5)). The necessary boundary conditions needed to solve the internal gas phase temperature Equation (13) are shown in Figure 5. These boundary conditions take into account conduction, convection, and radiation energy and establish internal tank surface temperatures on the top dome, liquid surface, and side walls.

The tank top dome temperature is established by Equation (14) which relates the solar flux to the sky reradiation, external wind convection, dome conduction, and dome temperature change.

$$Q_{\text{solar}} * E_{\text{do}} = Q_{\text{sky}} + Q_{\text{conv}} + Q_{\text{dome}} + (\rho L C_p) dT_{\text{do}}/dt \quad (14)$$

The solar radiation, Q_{solar} , is a function of many tank external variables. Variables such as clear sky to hazy sky ratio, day of the year, time of day, latitude, altitude, and emissivity of the tank external surface, E_{do} , are extremely significant in predicting the net incident solar radiation flux on a tank external surface. The instantaneous value of Q_{solar} can be predicted from the relationships found in Duffie and Beckman (1980) or could be supplied to the computer program from field data.

The sky reradiation energy flux, Q_{sky} , can be predicted by Equation (15):



TCP DOME (A), LIQUID SURFACE (B), HOT WALL (C)

FIGURE 5

Energy Equation Boundary Conditions

$$Q_{sky} = \sigma E_{do}(T_{do}^{**4} - T_{sky}^{**4}) \quad (15)$$

In Equation (15) the outside dome temperature, T_{do} , will vary with time of day as a result of solving Equation (14). The effective sky temperature, T_{sky} , is a function of daily ambient air temperature and can be computed from equations as given in Duffie and Beckman (1980).

The convective heat loss to the ambient air is given by Equation (16).

$$Q_{conv} = U(T_{do} - T_{air}) \quad (16)$$

The convective energy loss flux is equal to the heat transfer coefficient times the difference between the outside dome temperature, T_{do} , and the ambient air temperature, T_{air} . The heat transfer coefficient, U , is a function of tank size and wind velocity as given in Duffie and Beckman (1980).

The energy that conducts from the outside dome surface to the inside dome surface, Q_{dome} , is given by Equation (17):

$$Q_{dome} = (T_{do} - T_{di}) / (L_d / K_d + L_i / K_i) \quad (17)$$

Equation (17) contains the dome metal thermal conductivity, K_d , and the dome metal thickness, L_d , along with thermal conductivity and thickness of any insulation. Equation (17) essentially relates the inside dome temperature, T_{di} , to the outside dome temperature, T_{do} . The equations expressing the wall external and internal temperatures are similar to Equations (14), (15), (16) and (17) by replacing subscripts d with w .

The radiation energy fluxes are calculated simultaneously by Equation (18) in order to determine the inside dome, wall, and liquid surface temperatures.

$$Q_{rad1} = (J_1 - J_2) * F_{12} + (J_1 - J_3) * F_{13} \quad (18)$$

$$Q_{rad2} = (J_2 - J_1) * F_{21} + (J_2 - J_3) * F_{23}$$

$$Q_{rad3} = (J_3 - J_1) * F_{31} + (J_3 - J_2) * F_{32}$$

Equation (18) relate the net radiation leaving a surface to the radiosity, J , of the surfaces and the view factors, F , of the surfaces. The subscripts 1, 2, and 3 refer to the dome, wall, and liquid surfaces respectively.

The view factors are determined from the following relationships:

$$F_{13} = 1 - .62*H/R + .158*(H/R) * (H/R-1) \quad (19)$$

$$F_{31} = F_{13}$$

$$F_{12} = 1 - F_{13}$$

$$F_{32} = F_{12}$$

$$F_{21} = F_{32}*R/(2*H)$$

$$F_{23} = F_{21}$$

In Equation (19) H is the tank height and R is the tank radius. The values of the radiosities are calculated by Equation (20):

$$J_1 = (E_1*G_1 + (1-E_1)*(F_{12}*J_2 + F_{13}*J_3))/(E_1 + (1-E_1)*(F_{12} + F_{13})) \quad (20)$$

$$J_2 = (E_2*G_2 + (1-E_2)*(F_{21}*J_1 + F_{23}*J_3))/(E_2 + (1-E_2)*(F_{21} + F_{23}))$$

$$J_3 = (E_3*G_3 + (1-E_3)*(F_{31}*J_1 + F_{32}*J_2))/(E_3 + (1-E_3)*(F_{31} + F_{32}))$$

The values of G_1 , G_2 , and G_3 are $\sigma*T_{di}^4$, $\sigma*T_{wi}^4$, and $\sigma*T_1^4$. The Equations (18), (19) and (20) were obtained from Incropera and Dewitt (1981).

An energy balance at the inside dome surface then relates the Q_{dome} to the radiation leaving the dome and to the energy of conduction leaving the dome and flowing inside the tank;

$$Q_{dome} = Q_{rad1} - K_g*dT_g/dz \quad (21)$$

The second term in Equation (21) is the conduction of energy into the gas space at the dome. The equation for the wall energy is the same as Equation (21) with the subscripts changed from dome to wall and the temperature gradient taken in the horizontal plane.

The metal temperature distortion involved where the top dome and wall intersect was disregarded in the model for the following reasons: Using a cooling fin analogy, 90 percent of the temperature distortion caused at the intersection is recovered by the metals within 4 inches of the intersection. Similarly, the wall metal temperature distortion involved where the liquid basin and the wall intersect was also disregarded by using the same cooling fin analogy. The liquid basin temperature was assumed not to distort near the wall/basin intersection because of the large size of the basin.

The liquid surface energy balance relates the net radiation flux with the conduction fluxes into the gas and liquid phases together with the energy needed by the evaporating materials from the liquid surface:

$$0 = Q_{rad3} - K_g \cdot dT_g/dz - K_l \cdot dT_l/dz + \sum N_i \cdot \lambda \quad (22)$$

The following procedure is used by the computer model to establish the solar fluxes on the top dome and on each section of the walls. The walls were divided into 42 vertical sections so that the direction of solar energy with time of day could be taken into account. The equations needed to establish the solar insolation on the tank exterior surfaces were obtained from Duffie and Beckman (1980).

1. The latitude angle of the tank location is specified by the user, ϕ . ϕ is positive north of the equator.
2. The day of the year is specified by the user, N_{day} .
3. The earth angle of declination is calculated, δ .

$$\delta = 23.45 \cdot \sin(360 \cdot (284 + N_{day}) / 365)$$
4. The sunset angle is calculated, W_s , by:

$$\cos(W_s) = -\tan(\delta) \cdot \tan(\phi)$$
5. The number of daylight hours is calculated, N ; $N = 2 \cdot W_s / 15$

6. The time of dawn and sunset are calculated; $t_{dawn} = 12 - N/2$
 $t_{set} = 12 + N/2$
7. At a specific time of day set the solar angle, W ;
 $W = W_s + 15 * (\text{time} - t_{dawn})$
8. Calculate the angle of incidence or the angle between the beam radiation on a horizontal surface and the normal to that surface, θ_z , $\cos(\theta_z) = \sin(\delta) * \sin(\phi) + \cos(\delta) * \cos(\phi) * \cos(W)$
9. Calculate the hourly extraterrestrial radiation on a horizontal surface,
 $I_o = 414 * (1 + .033 * \cos(360 * N_{day} / 365)) * (\sin(\phi) * \sin(\delta) + \cos(\phi) * \cos(\delta) * \cos(W))$
10. Calculated beam radiation, T_b ; $T_b = a_0 + a_1 * \exp(-k / \cos(\theta_z))$ where a_0 , a_1 and k are functions of altitude and day of year
11. Calculate diffuse radiation, T_d , $T_d = .271 - .2939 * T_b$
12. Specify the clearness ratio which is the ratio of the clearness of the sky to that of the sky on a perfectly clear day, I_{clear} .
13. Calculate the diffuse fraction of total radiation, I_{dI} ,
 $I_{dI} = 1 - .1 * I_{clear}$ if $I_{clear} < .48$, $I_{dI} = 1.1 + .0396 * I_{clear} - .789 * I_{clear}^2$ if $.48 < I_{clear} < 1.1$, $I_{dI} = .2$ if $I_{clear} > 1.1$
14. Calculate the total radiation on a horizontal surface, I_{hor} ,
 $I_{hor} = I_{clear} * (T_b + T_d) * I_o$
15. Calculate the diffuse radiation, I_d , $I_d = I_{dI} * I_{hor}$
16. Calculate total beam radiation, $I_b = I_{hor} - I_d$
17. Select a portion of the wall and calculate the angle from the normal of the surface to the meridian, Γ ,

18. Calculate the angle of solar incidence with the normal of the surface, θ , $\cos(\theta) = -\sin(\delta)\cos(\phi)\cos(\gamma) + \cos(\delta)\sin(\phi)\cos(\gamma)\cos(W) + \cos(\delta)\sin(\gamma)\sin(W)$

19. Calculate the total solar energy on that particular vertical surface, I_{vert} , $I_{vert} = I_d + I_b\cos(\theta)/\cos(\theta_z)$

By using this procedure, the solar energy that is incident on the top dome and on 42 different positions on the side walls can be estimated for a storage tank located at a specific place and on a specific day of the year.

Flashing

The mathematical model takes into account the possible flashing of crude oil as high pressure feed stocks are reduced to atmospheric conditions. The crude is identified with 14 possible hydrocarbon species together with 4 possible dissolved gases and may or may not contain liquid water and steam under high pressure. The crude is analyzed at a specified temperature and pressure by the computer program to determine the vapor and liquid phase amounts and compositions. This analysis allows the crude energy content to be established so that when the crude pressure is dropped to ambient, the resulting flashed vapor and liquid mixture has the same energy content as the specified high pressure crude. This adiabatically flashed crude is assumed to be separated into pure vapor and pure liquid streams. These streams can then be routed to a storage tank at the user's discretion. For example, the liquid stream is sent to a specific location in the tank's liquid basin while the vapor stream may be routed to a specific top dome location, or to the liquid basin area, or it may simply bypass the tank altogether.

Specifically, the 14 hydrocarbon species that identify the crude composition are; methane, ethylene, ethane, propylene, propane, isobutane, n-butane, isopentane, n-pentane, n-hexane, n-heptane, n-octane, n-nonane, and

decane. Materials that are higher in molecular weight than n-decane will be lumped together and designated as n-undecane plus; the 4 hydrocarbon soluble gases incorporated in the program are; carbon dioxide, hydrogen, hydrogen sulfide, and nitrogen. The vapor liquid equilibrium constants (K values) for the hydrocarbon species were obtained from the DePriester charts (DePriester 1953) and for the dissolved gases from Edmister and Lee (1983).

The algorithm used by the program to flash high pressure crude is as follows:

1) The user specifies the temperature, pressure, and overall mole fractions of all hydrocarbon and gas species present in the crude oil mixture ($Z(i)$). Also the total moles of hydrocarbon plus dissolved gas, F_{hc} , and total water (liquid plus steam), F_w , must be user specified.

2) At the specified feed temperature the program calculates the theoretical bubble point pressure of the hydrocarbon/gas/ H_2O mixture. If the calculated bubble point pressure is greater than the specified crude pressure, then the feed stock is two phased and a vapor/liquid equilibrium calculation is run. If the bubble point pressure is less than the specified feed pressure, then the feed stock is all liquid and a calculation of vapor/liquid equilibrium is not run. If the bubble point pressure is less than atmospheric pressure, then the feed is all liquid and will still be liquid, even after reducing the pressure to atmospheric so the flashing step is bypassed.

3) The vapor/liquid equilibrium calculation of the crude at the high specified pressure requires the following steps:

A) The vapor pressure of the hydrocarbon is established by subtracting the vapor pressure of water from the total pressure if water is present.

$$P_{hc} = P_{total} - P_w$$

23

B) The equilibrium $K(i)$ values are calculated as functions of the temperature and hydrocarbon pressure by interpolation amongst the $K(i)$ data values.

C) The quality of the hydrocarbon-only mixture, Q_{hc} , is assumed and the following expression is calculated;

$$\sum_i Z(i) / (Q_{hc} * (K(i) - 1) + 1) \quad 24$$

D) If expression 24 is not equal to 1, then return to C) and reguess Q_{hc} . If expression 24 is equal to 1, then proceed to F).

F) Calculate the hydrocarbon-only liquid phase composition, $X(i)$, of each hydrocarbon and dissolved gas species;

$$X(i) = Z(i) / (Q_{hc} * (K(i) - 1) + 1) \quad 25$$

G) Calculate the hydrocarbon-only vapor phase composition, $Y(i)$, of each hydrocarbon and dissolved gas species;

$$Y(i) = K(i) * X(i) \quad 26$$

H) The steam quality is calculated:

$$Q_w = Q_{hc} * P_w * F_{hc} / (P_{hc} * F_w) \quad 27$$

If Q_w is greater than 1, thereby indicating that all the water is vapor, the program outputs a message that the wash tank is dry of liquid water and stops.

I) The total energy of the composite hydrocarbon/gas/ H_2O mixture is calculated using as a basis feed liquid at the feed temperature.

4) Flashing of the crude oil feed proceeds as follows:

A) The pressure of the crude is reduced to atmospheric.

B) The resultant temperature of the flashed crude is assumed.

C) Step 3) above is repeated to establish Q_{hc} , Q_w and the energy content of the composite hydrocarbon/gas/ H_2O mixture.

D) The energy of the flashed crude mixture is compared to that of the original high pressure crude mixture. If the energies are not equal, then step 4B is returned to and the temperature of the flashed crude is once again assumed. If the energies are equal, the vapor and liquid streams are routed to the wash tank. From this point on the program continues with emissions calculations.

Model Simulations

The following examples of crude storage and treatment tanks identified the sensitivity of process variables on predicted hydrocarbon emissions by a single phenomenon and case study approach. The single phenomenon simulations involved only one of the emitting mechanisms (i.e., working, breathing, or flashing). The case study approach analyzed the effect of model input variables on two field tests tanks from the WOGA study selected by ARB in which all three emitting mechanisms were involved simultaneously (memo Metzger to Beckman 5/22/86). The single phenomenon simulations used large variable movements to identify the largest as reasonable effects on emissions, while case studies used variable movements that were thought to be a reasonable error in the variable value.

Breathing Loss

The breathing loss variables that were investigated in this simulation together with their effects on emissions are listed in Table 1. A base case was selected from the 1977 WOGA tank emissions test (Engineering Science 1977) to represent variable values similar to a typical crude tank operation. The Aminoil 25697 tank was selected primarily because it was the

first tank listed, which contained a crude analysis. The tank was 29 feet in diameter with a 9 ft liquid outage. The crude analysis used is shown in Table 2. Emission values shown in Table 1 were generated by moving a designated variable from the base case value in a one-at-a-time manner. The base case will be described in detail together with phenomena-logical reasons to explain the emission responses to variable changes as shown in Table 1.

The BASE CASE variable settings are listed in Table 1. Figure 6 shows various tank temperatures together with dome vent velocity of the base case for a 24 hour period at terminal state. The temperatures shown include ambient, dome, east and west sides, and liquid surface. The ambient temperature was assumed to be sinusoidal with a maximum of 62 F occurring at 2:00 p.m. and a minimum occurring at 2:00 a.m. The side walls and the dome temperatures were forced to change by solar effects. As seen in Figure 6, the east wall rose in temperature extremely rapidly early in the morning and peaked at 120 F at 9:30 a.m. The dome achieved a maximum temperature at noon of 103F. In this case noon was solar noon at which time a maximum temperature would occur on a flat horizontal surface. The west wall achieved a maximum temperature of 123 F at 3:00 p.m. The west wall maximum temperature was greater than that of the east wall because of warmer ambient air temperatures in the afternoon as compared to the morning. The dome temperature did not achieve the wall temperature highs mainly because of the assumed low emissivity (high reflectivity) of the dome aluminum paint as compared to the higher emissivity paint on the walls. The liquid surface temperature resulted from the temperatures of the walls, dome, and bulk liquid. For this reason the maximum temperature of the liquid surface extends from 11:00 a.m. to 1:00 p.m. at 122 F.

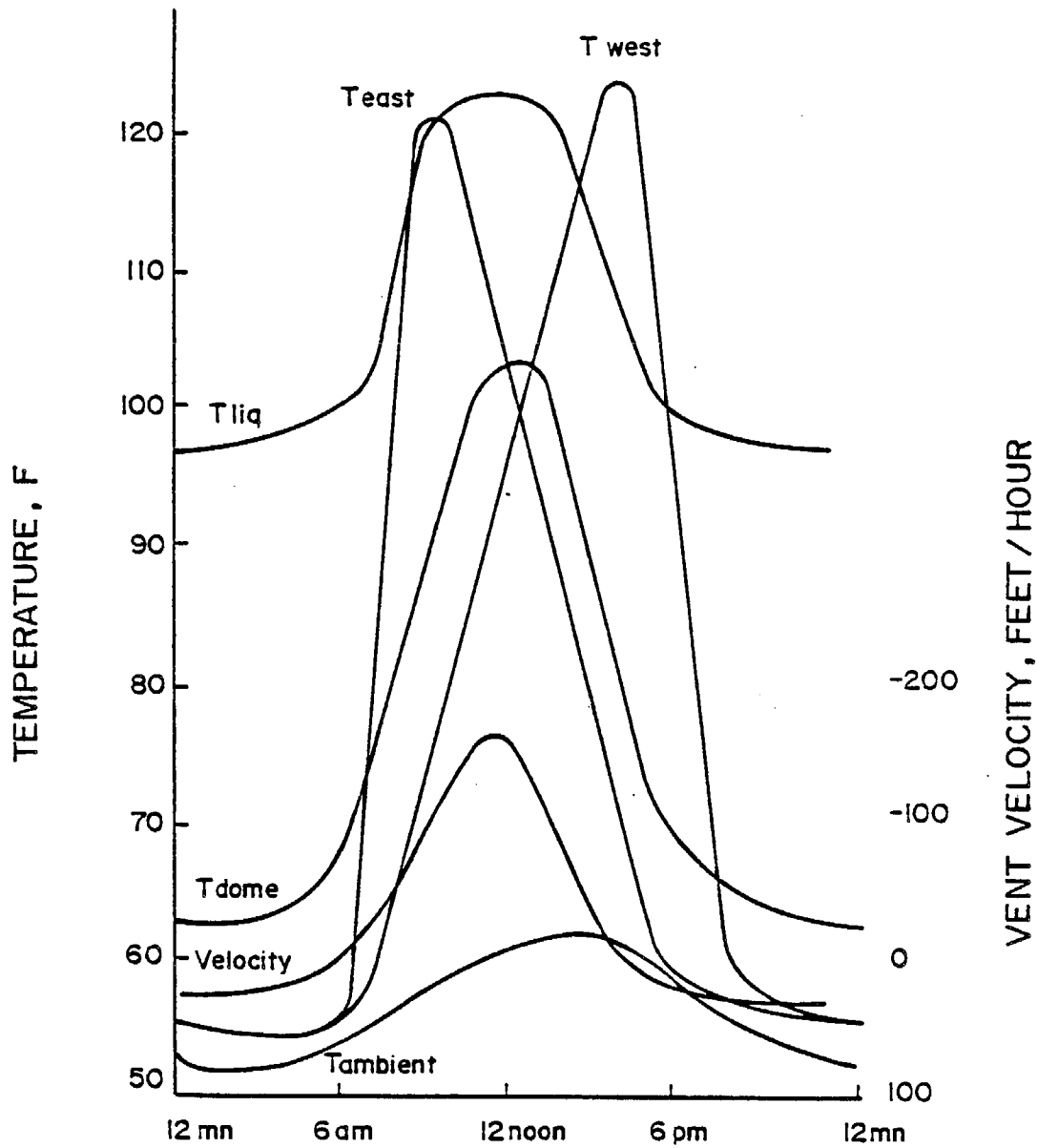


FIGURE 6

Temperature and Vent Velocity versus Time
in a Breathing Tank

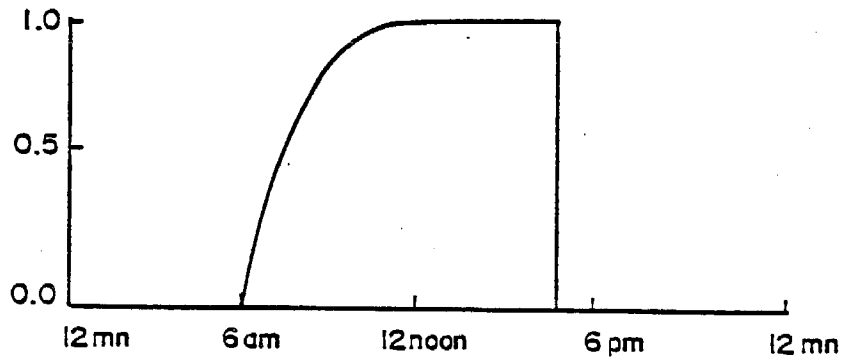
The vent velocity reflects the change in the thermal state of the gas head space inside the tank. Positive velocities indicate inhale while negative velocities indicate exhale and result in emissions. The vent velocities predominantly inhale at night and exhale during daylight hours. The vent velocity is essentially in an inhaling and constant rate from about 7:00 p.m. to 3:00 a.m. Because of the ambient air warming after 2:00 a.m. and the solar sun rise at 5:30 a.m., the vent velocity eventually switches from an inhale to an exhale condition at about 7:00 a.m. The exhale velocity increases and achieves a maximum value at noon and then declines to inhale at 4:30 p.m. After sunset at 6:30 p.m., the inhale velocity levels off repeating the cycle.

The composition of the gases at the vent are shown in Figure 7 along with vent velocity. The gas composition at the vent during inhale is essentially pure air. Inhale gas velocities are on the order of 20 ft/hr thereby preventing diffusion of hydrocarbons into the vent area. During exhale, a rise in hydrocarbon composition to a maxima requires about 5 hours. This time dependent rise is indicative of diffusion or minor mixing controlled transport of hydrocarbon vapors. If strong mixing induced by high gas velocities existed, the gases would then have been homogeneously mixed and the rise in hydrocarbon content of the exhale vent gases would have been immediate. The sharp rate of hydrocarbon composition reduction during inhale is once again a result of inlet vent velocities being high enough to deter species diffusion.

Table 3 lists gas volume inhaled and exhaled along with total pounds emitted during a 24 hour period at terminal state.

After the base case was established, the process variables were adjusted one-at-a-time to observe effects on daily emissions.

NORMALIZED CONCENTRATION $C_a/C_a \text{ max}$



VENT VELOCITY, FEET/HOUR

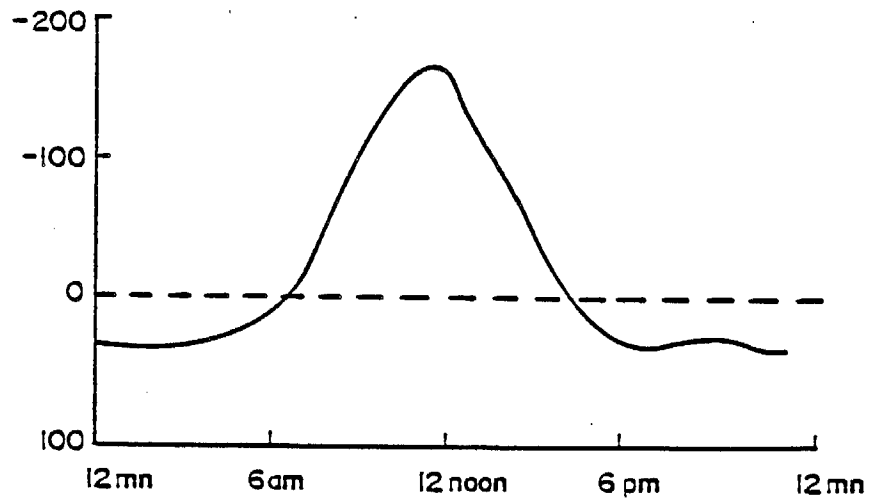


FIGURE 7

Vent Velocity and Vent Hydrocarbon Concentration versus Time

TANK DIAMETER was reduced from 29 ft to 25 ft resulting in a reduction in emissions to 77% of the base case value. This emission reduction is directly related to the dome plus side wall tank area reduction to 80% of the base case tank area. The reduction in tank area resulted in less solar pumping of the tank's internal gas space. Tank diameter is one of the major variables affecting breathing emissions investigated in this study. This variable had a percent emissions change per percent variable change of 1.5 (see Table 1).

The effect of paint color and condition quantified as EMISSIVITY was found to be a major variable since it dictated the net solar energy that would be adsorbed by the tank dome and wall external surfaces. The base case had a wall emissivity of 0.9 for light gray paint and a dome emissivity of 0.17 for diffuse aluminum paint. When the top dome emissivity was increased to 0.9, emissions increased by 62% over the base case value. The result of increasing dome emissivity allowed more solar energy to be adsorbed by the dome and thereby increased the dome temperature over that of the base case. The dome temperature ranged from 140 F to 55 F compared to the base case swing of 103 F to 62 F, thus increasing the thermal pumping action by 110% and resulting in increased emissions. When the side wall emissivity was reduced from 0.9 to 0.17, emissions were reduced by 38% of the base case value.

SIDE INSULATION having a 1.0 inch thickness and thermal conductivity of 0.02 Btu/ft hour °F was assumed resulting in a wall temperature swing of 36 F as compared to 51 F for the base case. Emissions were reduced by 15% of the base case value.

The DAILY AMBIENT TEMPERATURE CHANGE was increased by raising the daily high from 63 F to 80 F while leaving the daily low at 52 F. This increase

resulted in a 20% increase in emissions. By increasing the daily ambient temperature swing, the dome and wall temperature swings were forced to increase. The dome temperature change was 116 F to 62 F compared to the base case values of 103 F to 62 F. The wall temperatures changed an average of 132 F to 54 F compared to base case values of 123 F to 54 F. These increases in dome and wall temperature swings resulted in an increased thermal pumping of the tank gases.

The LIQUID SURFACE FILM HEAT TRANSFER THICKNESS was increased from 0.1 ft to 0.3 ft resulting in a 47% increase in emissions over the base case value. Since the bulk liquid temperature is 145 F and the dome and side walls are cooled, the liquid surface acts as a net radiator, thereby cooling below 145 F. The high and low liquid surface temperatures ranged from 110 F to 75 F compared to 122 F to 98 F for the base case. The liquid surface temperatures are lower than that of the base case due to the increased thickness of the liquid thermal boundary layer and to the fact that the liquid surface is a net radiator of energy. The reduction in the daytime high liquid surface by 12 F was different than the change in the nightly low by 23 F, resulting in an increase in the thermal pumping of the tank gases.

The LIQUID SURFACE MASS TRANSFER FILM THICKNESS was increased from 0.0001 ft to 0.1 ft resulting in an emissions decrease of 37% of the base case value. This increase in film thickness increased the resistance of the more volatile components which had higher mass diffusion fluxes than the less volatile components. For this case the emissions of methane were reduced by 78% of the base case value while emissions of hexane were unaffected. The size of both the liquid surface heat and mass transfer films were now assumed to be equal so the user need specify only one resistance thickness.

WIND VELOCITY was increased from 5 MPH to 20 MPH decreasing emissions by 31 % of the base case value. The effect of higher wind velocity was to change the heat transfer coefficient on the tank shell from 1.15 BTU/ft² hour F to 2.64 BTU/ft² hour F, allowing the convective term in the dome and wall energy balance to increase. This increase reduced the temperature change in the tank shell, thereby reducing the thermal pumping of the tank internal gases. The dome temperature swing for this case was 83 F to 58 F compared to the base case of 103 F to 62 F giving a ratio in swing of 0.61. The wall temperature swing for this case was 99 F to 52 F compared to the base case of 123 F to 54 F giving a swing ratio of 0.68. These ratios relate directly to the emissions reduction.

LIQUID COMPOSITION of methane through decane were reduced by 10% of the base case values, resulting in a 23% decrease in emissions. This decrease is a result of reduced vapor pressure of the liquid from 7.8 psi to 7.1 psi. Liquid composition is one of the major variables affecting breathing emissions investigated in this study. This variable had a percent emissions change per percent variables change of 2.3 (see Table 1).

VAPOR-LIQUID EQUILIBRIUM constants were reduced to 90% of the base case values, resulting in a 25% reduction in total emissions. This response is essentially the same as that exhibited by liquid composition reduction just discussed. Since the product of the vapor-liquid equilibrium constant and the liquid concentration determine the partial pressure of a volatile species, it is then expected a change in either variable should have a similar effect on emissions. Vapor/liquid equilibrium constant is one of the major variables affecting breathing emissions investigated in this study. This variable had a percent emission change per percent variable change of 2.5 (see Table 1).

VACUUM-PRESSURE vent settings were adjusted to 1.0 inches of water compared to 0.0 inches of water for the base case. Emission was reduced to 87% of the base case value because of the reduction in intake and emitted total gas volumes. A total of 2.0 inches of water pressure change in the gas outage space was calculated to be 30 cubic feet of gas, which would reduce the intake gas volume by approximately 10%.

LIQUID OUTAGE was set at 3 ft and 6 ft, resulting in emissions of 56% and 96% of the 9 ft base case emissions. Table 4 lists the total gas volume emitted, total air volume inhaled, and hydrocarbon mole fraction of the emitted air. Table 4 shows that as outage increased air intake volume increased because of the increase in tank shell area, thus increasing the solar pumping effect. This action tends to increase emissions. Table 4 also shows that the hydrocarbon content in the exhaust gas decreased with increased outage. This decrease in hydrocarbon composition results from increased distance of the saturated liquid surface from the top dome and from increased volume of air cloud, which is brought into the tank. Diffusion and velocity mixing mechanisms find it more difficult to move hydrocarbons into the air cloud thus reducing hydrocarbon content in the exhaling gas. Effects that both increase and decrease emissions resulted in a gradual increase in emissions for these cases.

GEOGRAPHIC LATITUDE was changed from 35 degrees north (Los Angeles) to 40 degrees north (Eureka), resulting in a 3.5% decrease in emissions of the base case. This decrease resulted from a decrease in the solar flux which, for instance, lowered the noon dome temperature from 102 F to 101 F.

ALTITUDE was changed from sea level to 1000 ft while ambient pressure remained unchanged, resulting in a 1.9% increase in emissions. This

increase in altitude increased the noon dome temperature from 102 F to 104 F.

The CLEARNESS INDEX was decreased from 0.9 to 0.7 making the day less clear causing the emissions to be decreased by 5.8% of the base case value. The reduction in the dome noon time temperature from 102 F to 99 F reduced the thermal pumping of the internal tank gases.

The DEW POINT TEMPERATURE, which is used in the calculation of the effective sky temperature, was increased from 30 F to 50 F causing a 0.4% increase in emissions. This dew point temperature increased the dome noon temperature from 102 F to 104 F but also increased the dome midnight temperature from 63 F to 65 F. Consequently, the tank stayed warmer, but the thermal pumping action did not change, resulting in essentially no change in emissions. This variable was removed from the model.

The GAS PHASE DIFFUSIVITY was doubled, resulting in a 36% increase in emissions compared to the base case. Increased emissions resulted because of the increased diffusion of hydrocarbons into the inhaled air cloud before the completion of the exhale phase. Methane emissions increased by 40% while decane emissions increased by only 20% as seen in Table 5.

DOME VENT LOCATION was changed from the center to the side edge of the dome, resulting in a 3% decrease in emissions. Some decrease in emissions was expected since the surface area of the air cloud was somewhat shielded by the side wall, thus reducing the hydrocarbon diffusion into the air cloud before exhale.

DOME VENT DIAMETER was decreased from 1.0 ft to 0.5 ft resulting in a 20% increase in emissions compared to that of the base case. Predominantly during inhale, the internal gas velocity just under the dome vent is upward moving because of its low density (low hydrocarbon content). As the vent

diameter was halved, the velocity of the inhale gas increased by a factor of four, which increased its downward inertial effect and result^{ed} in a suppression of the upward moving gas in the vent vicinity by a factor of approximately four. This velocity suppression allowed more hydrocarbon to diffuse into the vent area gases during inhale thus increasing emissions during exhale. Larger vent diameters than 1.0 feet for this case did not emit significantly less than the 1.0 feet case because of the diminishing effect of low vent velocities on gas movements inside the tank.

Working Loss

The working loss variables investigated in this study include amplitude and frequency of a saw-tooth wave used to describe liquid outage and the average liquid outage. A base case operation was specified, and a one-at-a-time variable movement from the base case was used to ascertain the variable effect on resultant emissions. Table 6 summarizes the variable movement and emissions relative to the base case. The base case selected comprised a liquid outage of from 7 ft to 9 ft with a period of 4 hour. The gas volume displaced by the liquid movement in the 29 ft tank was 1320 cubic feet per cycle. Table 6 shows that only 1040 cubic feet of gas was inhaled, which is less than the 1320 cubic feet because of the liquid surface evaporation rate during inhale. The exhale gas volume was 1600 cubic feet which contained 560 cubic feet of hydrocarbon and 1040 cubic feet of air.

The OUTAGE AMPLITUDE was changed from 2 ft (7 ft to 9 ft) to 4 ft (6 ft to 10 ft), resulting in a 93% increase in emissions over that of the base case. Table 6 shows that the inhale gas rate was about twice the base case value as it should have been and that the hydrocarbon content (mole fraction) in the exhale gas decreased from 0.35 to 0.34. This decrease in

hydrocarbon content in the exhale gas results from the increased diffusion path length into the larger air cloud.

The OUTAGE FREQUENCY was decreased by increasing the cycle period from 4 hour to 8 hour; this resulted in a 10% increase in emissions per cycle. This increase was a result from increased residence time of the air cloud inside the tank, allowing more hydrocarbons to diffuse into the cloud before exhale. Table 6 shows that the hydrocarbon mole fraction in the exhaust gas increased from 0.35 to 0.38.

The OUTAGE AVERAGE LEVEL was reduced from 8 ft (7ft to 9 ft) to 6 ft (5 ft to 7 ft) to result in a 3.5% increase in emissions. The emissions increased because of the reduced diffusion distance from the liquid surface to the top dome vent.

Flashing Loss

The flashing loss study investigated the effect on emissions by the following variables: pre-flash feed pressure, pre-flash feed temperature, water flow rate, hydrocarbon flow rate, and post-flash vapor tank feed location.

A base case was selected about which the variables were moved in a one-at-a-time method to observe the effect on emissions. The base case considered a pre-flash feed pressure of 24 psia, pre-flash feed temperature of 200 F, water feed rate of 400 lb moles/hour, hydrocarbon feed rate of 435 lb moles/hour, and a dome location for the post-flash vapor feed to the tank. Table 7 lists the qualities, post-flash temperatures, and hydrocarbon water emissions for the base case and all other flash cases considered in this study.

The PRE-FLASH FEED PRESSURE was increased from 24 psia to 26 psia causing a 24% decrease in emissions as compared to the base case. The

higher feed pressure reduced the hydrocarbon and water pre-flash quality thereby lowering the energy content of the feed. This lowered the post-flash qualities, thereby reducing emissions.

The PRE-FLASH FEED TEMPERATURE was increased from 200 F to 210 F, which increased emissions by 76% over that of the base case. By increasing the pre-flash temperature, the energy content and qualities of the pre-flash feed were increased. Post-flash qualities were increased as were emissions.

Reducing the WATER FEED RATE from 400 lb moles/hour to 360 lb moles/hour resulted in a slight decrease in emissions of 2.1%. This change only affected the pre-flash water quality in the pre-flashed feed which slightly reduced post-flash hydrocarbon to result in lower emissions.

The HYDROCARBON FEED RATE was reduced from 435 lb moles/hour to 400 lb moles/hour to effect a 10% reduction in emissions. This reduction in feed rate only slightly reduced the post-flash hydrocarbon quality. The emissions mainly reflect the 8% reduction in hydrocarbon feed rate.

When the POST-FLASH VAPOR FEED LOCATION was moved from the top dome location to the liquid surface, emissions were reduced to 95% of the base case value. The reduction in emissions was mainly because of vapor condensation at the cold liquid surface. Since the vapor was fed to the liquid surface vicinity, there was more intimate contact with the cool liquid surface than in the base case, which caused slightly increased condensation and reduced emissions.

TABLE 1
Variables Affecting Breathing Loss

Variable	Move		% Emission Change	% Emission* Change per % Variable Change
	From	To		
Tank Diameter	29 ft	25 ft	-23	1.5
Liquid Outage	9 ft	12 ft	15	0.5
Dome Emissivity	0.17	0.9	62	0.5
Wall Emissivity	0.9	0.17	-38	0.3
Side Insulation	0.0 in	1.0 in	-15	-0.1
Ambient temperature change	11 F	28 F	20	0.2
Liquid heat trans film	0.1 ft	0.3 ft	47	0.5
Liquid mass trans film	E-6 ft	E-4 ft	-27	-0.1
Wind Velocity	5 MPH	20 MPH	-31	0.3
Liquid composition	base	90% base	-23	2.3
VLE constant	base	90% base	-25	2.5
Press/vac vent settings	0/0	1 in/1 in	-13	0.0
Latitude	35 deg	40 deg	-3.5	-0.3
Altitude	0 ft	1000 ft	1.9	0.0
Clearness index	0.9	0.7	-5.8	0.2
Dew point Temperature	30 F	50 F	0.4	0.0
Gas phase Diffusivity	base	2 x base	36	0.5
Vent location	center	edge	-3.0	---
Vent diameter	1.0 ft	0.5 ft	20	0.3

*based on average variable value

TABLE 2
Crude Liquid Composition

Component	Mole Percent
Methane	0.16
Ethane	0.12
Propane	0.56
i-Butane	0.38
n-Butane	1.02
i-Pentane	0.80
n-Pentane	0.79
Hexane	1.43
Heptane	22.00
Octane	29.00
Nonane	23.00
Decane	9.00
Undecane +	11.55
Carbon Dioxide	0.19
<hr/>	
Total	100.00

TABLE 3
Base Case 24 hr Breathing Emissions

Gas Volume Inhaled	114 cubic ft
Gas Volume Exhaled	139 cubic ft
lbs emitted	1.78
lbs emitted (no methane/ethane)	0.90

TABLE 4
Liquid Outage Effect on Emissions

Outage feet	Gas Volume	Air Volume	Hydrocarbon Fraction in Emitted Gas
	Emitted STD ft ³ /24 hr	Inhaled STD ft ³ /24 hr	
3	46	32	.30
6	105	81	.22
9	139	114	.18

TABLE 5
Gas Phase Diffusivity Effect on Emissions

Component	Emissions/lbmols/24 hr		% Change
	Base Case	2 X Dim Case	
Methane	0.410	0.572	40
Ethane	0.0651	0.0895	37
Propane	0.104	0.141	36
i-Butane	0.0297	0.0394	33
n-Butane	0.0656	0.0860	31
i-Pentane	0.0198	0.0256	29
n-Pentane	0.0146	0.0188	29
Hexane	0.0090	0.0114	27
Heptane	0.0464	0.0570	23
Octane	0.0215	0.0258	20
Nonane	0.0029	0.00348	20
Decane	0.00017	0.000207	20
Carbon Dioxide	0.253	0.353	40

TABLE 6
Working Loss Emissions

Liquid Outage feet		Period hours	Total Gas Inhaled	Total Gas Exhaled	Hydrocarbon Fraction in Exhaled Gas
Low	High		ft ³ /cycle	ft ³ /cycle	
7	9	4	1040	1600	0.35
7	9	8	1010	1629	0.38
6	10	4	2099	3181	0.34
5	7	4	1030	1610	0.36

TABLE 7
Flashing Loss Emissions

Feed Press Psia	Feed Temp F	Water Feed Rate mol/hr	Crude Feed Rate mol/hr	Pre-Flash Quality		Post-Flash Quality		Emissions/24 hr lb moles	
				crude	H ₂ O	crude	H ₂ O	crude	H ₂ O
* 24	200	400	435	0.025	0.025	0.046	0.068	458	639
26	200	400	435	0.017	0.015	0.042	0.059	348	554
24	210	400	435	0.074	0.110	0.081	0.160	806	1503
24	200	360	435	0.025	0.028	0.045	0.075	448	634
24	200	400	400	0.025	0.023	0.045	0.062	412	582
**24	200	400	435	0.025	0.025	0.046	0.068	435	607

* Base Case

** Liquid surface post-flash vapor feed location

Case Study A (UNION 8826)

Case study A simulated emissions from the 1977 WOGA study UNION 8826 tank. The tank was working over a 24 hour period in the following manner: in the evening the liquid outage increased from 3 ft to 6 ft in one hour and then sat idle until day time when the outage gradually decreased to 3 ft by evening. A sensitivity analysis of variables effect on emissions is summarized in Table 8. Table 8 shows that total emissions per cycle of 22 lb agreed very closely with 21 lb as reported by WOGA. The predicted methane/ethane content of emissions was about 6 lbs per cycle compared to only 1.5 lbs reported by WOGA. Agreement would be closer if the equilibrium K value of methane could be reduced.

Tank diameter (variable 1 in table 8) was found to be the variable that most importantly affected emissions. Table 8 shows a value of 3.5 for % emission change per % variable change indicating that tank diameter was two to three times more important than any other variable in determining emissions.

Variable 10, the liquid surface film thickness resistance, was increased from 0.0001 ft to 1.0 ft showing a reduction in emissions from 22.1 lb to 3.5 lbs. This is because of the diffusion limitations in the liquid phase of species getting to the liquid surface for evaporation. This is the only variable in the emission model that is free to be set by the judgment of the user. A value of 0.0 feet for film thickness implies a well mixed liquid basin while a value of 1.0 feet models a stagnant unmixed liquid basin. Since a small resistance thickness of 0.001 feet gave a best match to the WOGA total emissions of 21 lb/cycle, it is apparent that UNION 8826 tank was mathematically well mixed.

Variable 6, outage amplitude, had a directly proportional effect on emissions. As the pumped volume rate increased by 33% (3 ft to 4 ft), emissions increased by 40%. This movement in emissions shows that working effects and not breathing effects dominated emission results.

TABLE 8
Case Study A (Union 8826)
Predicted Emissions

			Total Emissions <u>lb/cycle</u>	Emissions (no methane/ ethane) <u>lb/cycle</u>	<u>%Emission Change/ %Variable Change</u>
WOGA DATA			21	19.2	
Base Case			22.1	16.4	
<u>Variable</u>	<u>Value</u>	<u>Base Value</u>			
1. tank diameter, ft.	16	15.5	24.6	18.5	3.5
2. vent diameter, ft.	1.1	1.0	22.5	16.8	0.2
3. vent location	11/13	11/11	23.0	17.2	---
4. ambient pressure, psi	14.0	14.7	23.4	17.1	1.2
5. vac/press, in	0/0	1.5	24.9	18.2	0.1
6. outage, ft	3/7	3/6	31.1	23.2	1.2
7. liquid temp, °F	70	65	20.8	14.8	-0.8
8. feed composition	.9Z	Z	19.2	14.4	-1.3
9. feed molar density	.236	.215	23.9	17.6	0.8
10a. film thickness, ft.	.001	.0001	21.0	17.0	0.0
10b. film thickness, ft.	.01	.0001	18.7	14.9	0.0
10c. film thickness, ft.	.1	.0001	12.3	8.6	0.0
10d. film thickness, ft.	1.	.0001	3.5	3.0	0.0
11. daily high temp, °F	85	80	22.4	16.8	0.2
12. solar clearness	.5	.7	22.1	16.7	0.0
13. diffusivity	2D	D	24.0	18.3	0.1
14. K	1.1K	K	25.5	19.1	1.5
15. outside emissivity	.3	.17	22.1	16.4	0.0
16. inside emissivity	.8	.9	21.9	16.3	-0.3

Case Study B (EXXON 410)

Case study B simulated emissions from the 1977 WOGA study EXXON 410 tank. The tank was rapidly being worked and had dominant flashing effects. Although the tank was working with a 1 ft amplitude and 0.6 hour period, the tank never inhaled; in fact only variables associated with the flashing phenomenon influenced predicted emissions.

Table 9 shows the effect of flashing variables on emissions. In general the predicted total exhaust gas was 70% greater than WOGA data, total emissions were in excellent agreement, but propane+ emissions were only 26% of the data values. The main variables which most importantly affect total emissions were found to be feed temperature (variable 1), feed molar density (variable 4), feed methane content (variable 6), and feed propane to decane content (variable 7). Table 9 shows that in order to more closely predict the WOGA data emission values, a move in a major variable value would have to reduce total off gas, leave unchanged total emissions, and increase propane + emissions. Unfortunately, movements in variables 1, 4, 6 and 7 accomplished only one of the goals and violated the other two.

Liquid film thickness had a minor effect in reducing emissions because of the fact that emissions result from flashing not working effects. Reducing the feed pre-flash methane content (variable 6) from 0.0122 mole fraction to 0.01 mole fraction reduced overall exhaust gas but also reduced total emissions. Doubling the feed pre-flash propane through decane content increased both total exhaust gas and emissions. Reduction in methane vapor/liquid equilibrium constant to 80% of base case value resulted in reductions in total off gas and emissions. In order for the mathematical model to more closely agree with WOGA data for this case study, a combination of WOGA data adjustment and possibly model K values must be used.

TABLE 9
Case Study B (Exxon 410)
Predicted Emissions

	<u>total</u>	<u>emissions</u>	<u>flash quality</u>		<u>%Emission Change per %Variable Change</u>			
	<u>gas out</u>	<u>lb/day</u>	<u>crude</u>	<u>water</u>				
	<u>ft³/day</u>	<u>total</u>	<u>propane+</u>					
WOGA DATA	35,000	1518	963	--	--			
Base Case	59,600	1560	288	.0114	.00694			
<u>Variable</u>	<u>Value</u>	<u>Base</u>						
1. feed temp, °F	165	170	55,300	1487	272	.0113	.00599	1.6
2. feed pressure, psi	45	49.7	59,400	1575	291	.0114	.00694	-0.1
3. tank liq tem, °F	150	160	59,800	1519	259	.0114	.00694	0.4
4. feed molar density	0.17	0.157	63,900	1699	311	.0114	.00724	1.1
5. film thickness, ft	.1	.0001	59,100	1487	251	.0114	.00694	0.0
6. feed methane	.01	.0122	49,200	1180	236	.0093	.0059	1.3
7. feed C3 to C10	2B	B	93,600	4360	216	.0183	.010	1.8
8. methane K	.8K	K	56,000	1424	268	.0107	.0065	0.4

Central Processing Unit (CPU) Time Reduction Study

This phase of the model development focused on reducing the central processing unit (CPU) running time to better accommodate ARB computer hardware.

A breathing emissions base case was established which required 4 cycles to achieve 95% terminal state emission using 211 seconds CPU time. This was the same base case that was used for the single phenomenon study. The computer used was an IBM 3081 Processor Complex Model Group K with capable 32 megabytes of main memory. Three efforts made some impact on CPU reduction - reduced excessive convergence loops, established dimensionless composition, and start time of day. Reduction in CPU time is summarized in Tables 10 and 11.

Table 10 shows the CPU reduction by convergence relaxation and by dimensionless concentration. The convergence relaxation merely involved relaxing all convergence loops in the program without varying any outputs by more than 1% of the base values. CPU time was reduced to 183 seconds by this technique. The dimensionless concentration method involved defining a new concentration variable, ϕ , which was the ratio of the gas phase concentration, C_i , at any point in the gas space to the concentration of that species at the liquid surface just below the point, C_{i_s} , so $\phi = C_i/C_{i_s}$. In this manner $\phi = 1$ for all composition species at every point on the liquid surface. When the differential equation together with all boundary conditions was put into dimensionless form, only the gas phase diffusivity remained specific to each species; therefore, the dimensionless equation was solved only twice - once with methane diffusivity and once with octane diffusivity. By interpolating using values of species diffusivity, the gas phase concentrations for all 13 species were calculated. Table 11 shows

that by using the dimensionless composition method with relaxed convergence, CPU time was reduced to 147 seconds.

Table 11 shows the effect of start time and the number of cycles on prediction of terminal state emissions. The simulated tank was assumed air saturated in hydrocarbon species and the simulation was started at the beginning of the intake portion of the thermal cycle (3 p.m.). In this manner air was brought into the tank immediately to achieve terminal state more rapidly than the runs of Table 10. Table 10 runs were started at 3 a.m. which was the start of the exhaust portion of a thermal cycle. The starting time of 3 a.m., which is typified by slowly changing temperatures, was originally used to avoid possible numerical instabilities at the program start. It was found that the 3 p.m. starting time also gave no numerical instability problems.

Table 11 shows that terminal state emissions are rapidly achieved. After one cycle requiring 39 seconds of CPU time, 91% of the final terminal state emissions was achieved. Two cycles requiring 75 seconds CPU time came within 94% of terminal state emissions. After three cycles requiring 111 seconds, terminal state condition was achieved.

Table 10

Central Processing Unit (CPU) time reduction using as a basis 4 cycles
(95% terminal state emissions) starting at 3 a.m.

<u>Case</u>	<u>CPU, sec</u>	<u>% of base case</u>
base case	211	100
reduced convergence	183	87
dimensionless gas concentration	147	70

Table 11

Central Processing Unit (CPU) time reduction
using 3 p.m. starting

<u>Cycle</u>	<u>CPU, sec</u>	<u>% of 211 base</u>	<u>emissions, lb/cycle</u>	<u>% to terminal state</u>
1	39	18	9.0	91
2	75	36	9.3	94
3	111	53	9.7	98
4	147	70	9.9	100
5	183	87	9.9	100

Computer Program Methodology

The program inputs and outputs have been intended to be "user friendly" as much as possible; variable units tend to be in feet, degrees Fahrenheit, miles per hour, Barrel/day, psi, and inches of water pressure settings.

Briefly the inputs as per memo Metzger to Beckman 5/22/86 include:

- 1) tank diameter, height, and outage in feet
- 2) ambient, feed, and initial tank gas temperatures in °F
- 3) wind velocity in mph
- 4) water and crude throughput in BBl/day
- 5) feed composition in either mole fraction or weight fraction
- 6) crude feed and pressure in psi
- 7) pressure and vacuum valve settings in inches of water

In addition to these requested inputs the program has been developed to include daily changes in daily ambient high temperatures, daily ambient low temperature, daily clearness (for solar radiation), and daily wind velocity for an eight day period. These events represent uncontrollable variables in the desire of ARB to monitor hydrocarbon emissions from field test tanks. All other variables are first day established and remain as such for the duration of the simulation.

The output format includes the following features:

- 1) complete data echo
- 2) feed bubble point pressure or vapor pressure in psi
- 3) vapor pressure of the hydrocarbon only in the bulk tank liquid at
bulk tank liquid temperature in psia
- 4) time of day and cycle number

- 5) tank gas phase composition profile for each component in both weight and mole fraction at any specific vertical plane
- 6) vent gas emission rate in SCFM
- 7) total emission compositions in both weight and mole fraction for each emitting vent
- 8) emission not including methane and ethane in both weight and mole fraction for each emitting vent
- 9) emission rate in lbs/hr for each vent
- 10) emission rate not including methane and ethane in lbs/hr for each vent
- 11) cumulative gas emitted from start of cycle for each vent in SCF
- 12) tank internal gas temperatures on the vertical east/west plane through the tank center in °F
- 13) total cumulative hydrocarbon emissions per cycle in lbs for each emitting vent
- 14) total cumulative hydrocarbon emissions per cycle not including methane and ethane in lbs for each emitting vent.

It was felt that since 90% of the printout was associated with tank gas phase composition (item5), the user may select to suppress or delete item 5 printing (see input format listing card #25).

The computer program was compartmentalized into six distinct sections to facilitate the logical ordering of tasks.

The sections are:

- Section 1: DATA BLOCK
- Section 2: READ/ECHO
- Section 3: INITIALIZATION

Section 4: FLASH
Section 5: MAINTIME
Section 5a: TIME RESET
Section 5b: GAS VELOCITIES
Section 5c: GAS COMPOSITION
Section 5d: EMISSIONS
Section 5e: GAS TEMPERATURES
Section 6: FUNCTION VLE

Basically Section 1 contains the values of physical property variables such as the vapor/liquid equilibrium constants as a function of temperature and pressure, gas and liquid phase diffusivities, species molecular weights, species names, liquid phase heat capacities, and heats of vaporization. These values have been preset but may be altered at the users discretion. The values of the vapor/liquid equilibrium constant, K, for each species at three different temperatures and pressures that are used by the program are listed in Table 12. The value of K for each hydrocarbon was obtained from the DePriester charts (DePriester 1953) while the value of K for the dissolved gases such as nitrogen, hydrogen, hydrogen sulfide, and carbon dioxides were obtained from Edmister and Lee 1983. These values may be updated by results of experimental work being done at UC Davis.

Section 2 the READ/ECHO section is responsible for all variable values that must be read into the program.

The following card by card input list discussion is meant to guide the user in data input selection. The discussion will include details on cases involving working, flashing, and breathing effects. A program listing is included in the Appendix so that the user may reference directly to it. The

user should note that all inputted numbers must be followed by a decimal point in a ten space input window. The data cards are 80 spaces long so that a maximum entry of 8 numbers can be inputted on one line.

Card #1

Card #1 is the run identification, the user may enter any numbers or letters which will label the output.

Card #2

Enter tank diameter (feet) and total tank height (feet).

Card #3

Enter the number of emitting (output) dome vents. The program accepts a maximum of two.

Card #4

This is emitting vent #1, enter its diameter (feet), X and Y coordinates of its location (see Figure 8). If there is a second emitting vent, use a separate card for its information.

Card #5

Enter ambient pressure (psia), pressure and vacuum vent settings (inches of water)

Card #6

Enter diameter (feet) and XY coordinates of vapor post-flash vent (see Figure 8). Also enter 0 if a feed flash vapor is not to be sent to the tank, 1 if feed flash vapor is introduced to the top dome of the tank and 2 if feed flash vapor is introduced to the liquid surface. If there is no flashing of the feed, enter only 0 for the vent diameter.

TABLE 12
Program Assumed Vapor/Liquid
Equilibrium K Values

Component	50°F				100°F				200°F			
	14.7 psia	50 psia	200 psia	14.7 psia	50 psia	200 psia	14.7 psia	50 psia	200 psia	14.7 psia	50 psia	200 psia
Methane	120.	39.	11.	175.	44.	13.	230.	61.	17.			
Ethylene	27.	10.	2.9	49.	15.	4.4	86.	26.	7.7			
Ethane	16.	5.4	1.8	34.	9.3	2.9	68.	18.	5.3			
Propylene	5.4	2.2	0.6	13.	3.8	1.2	33.	8.7	2.7			
Propane	4.6	1.8	0.53	11.	3.3	1.0	29.	7.8	2.4			
iso-Butane	1.7	0.66	0.22	4.4	1.4	0.46	14.	4.0	1.3			
n-Butane	1.2	0.45	0.15	3.4	1.0	0.34	13.	3.3	1.0			
iso-Pentane	0.42	0.17	0.058	1.3	0.44	0.15	5.8	1.6	0.5			
n-Pentane	0.3	0.12	0.045	1.0	0.34	0.12	4.5	1.3	0.44			
n-Hexane	0.09	0.003	0.015	0.35	0.12	0.046	1.9	0.62	0.21			
n-Heptane	0.025	0.012	0.0052	0.12	0.045	0.019	0.86	0.29	0.10			
n-Octane	0.0085	0.0046	0.0023	0.046	0.018	0.0083	0.4	0.14	0.05			
n-Nonane	0.0022	0.0013	0.0003	0.013	0.006	0.003	0.15	0.056	0.023			
n-Decane	0.0005	0.00015	0.00004	0.0036	0.0017	0.0008	0.059	0.0023	0.009			
Carbon Dioxide	90.	28.	7.8	90.	28.	7.8	130.	41.	11.			
Hydrogen	650.	180.	48.	650.	180.	48.	600.	160.	46.			
Hydrogen-Sulfide	27.	9.5	3.1	27.	9.5	3.1	47.	17.	5.2			
Nitrogen	650.	180.	48.	650.	180.	48.	600.	160.	46.			

Card #7

Enter the number of liquid surface locations (outage) versus time data sets and the period of a cycle (hours). If the outage is not changing with time, the same outage must be entered at zero time and at final time. The last outage time is taken as the end of simulation. If no entry is given for the cycle period, the program assumes 24 hours.

Card #8

Enter liquid outage (feet) and time (hours) as a pair sequentially from time of zero to final time.

Card #9

Enter crude feed temperature (°F), crude feed pressure (psia) and tank bulk liquid temperature (°F). If a flash is to occur, the feed temperature and pressure must be at the pre-flash condition. Specify the tank bulk liquid temperature. If the tank bulk liquid temperature is not to be specified, enter 0 and the program will assume it to be the crude feed temperature if no flashing occurs or will set it to be the post-flash temperature if flashing occurs.

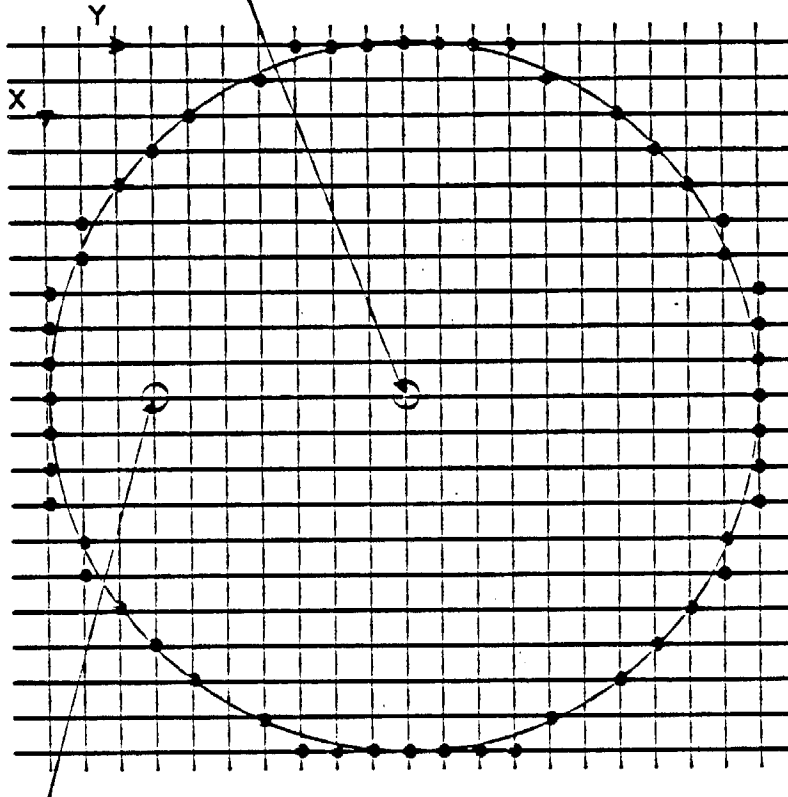
Card #10

Enter water feed rate (BBls/day)

Card #11

If the crude oil composition is in mole fraction, enter 1.0. If in weight fraction, enter 2.0.

EXAMPLE
(TOP EMITTING VENT X=11 Y=11)



EXAMPLE
(TOP DOME POST-FLASH VAPOR VENT X=11 Y=4 Z=1)

FIGURE 8

Example location of
vent ports

Card #12

Enter composition of crude feed on a water free basis (hydrocarbons and dissolved gases). Do not enter water. Enter in the order of: methane, ethylene, ethane, propylene, propane, i-butane, n-butane, i-pentane, n-pentane, n-hexane, n-heptane, n-octane, n-nonane, n-decane, carbon dioxide, hydrogen, hydrogen sulfide, and nitrogen.

Card #13

Enter crude oil feed rate (BBls/day) at 60°F.

Card #14

Enter hydrocarbon liquid density in lb moles/cu ft. at 60°F.

Card #15

Enter assumed liquid film resistance thickness in feet. This thickness is used for both heat and mass transfer from the bulk liquid to the saturated gas just above the liquid surface. A value of 0.0 feet gives no resistance, while a value of 0.1 feet is significant.

Card #16

Enter insulation thickness (feet) of any insulation on the top dome and side walls. If no insulation is present, enter 0., 0..

Card #17

Enter emissivity of top dome both outside and inside the tank.

Card #18

Enter emissivity of side walls both outside and inside the tank.

Card #19

Enter the tank internal initial gas temperature (°F) from top dome to liquid surface.

Card #20

Enter latitude (degrees), altitude above sea level (feet), day of the year, time of day to start cycle (24 hour clock).

Card #21

Enter ambient daily high (°F). There is capability of entering this information differently for as much as an eight day simulation. If only one entry is given, the program assumes this one value for all days.

Card #22

Enter ambient daily low temperature (°F). A capability exists of entering this information differently for up to an eight day simulation. If only one entry is given, the program assumes this one value for all days.

Card #23

Enter clearness index. There is capability of entering this information differently for as much as an eight day simulation. If only one entry is given, the program assumes this one value for all days.

Card #24

Enter wind velocity (MPH). There is capability of entering this information differently for up to an eight day simulation. If only one entry is given, the program assumes this one value for all days.

Card #25

If you do not want tank gas compositions printed, enter .0; if you want tank gas compositions printed at a specific time, enter the time (1 to 24), if you want tank gas compositions printed at all times enter 25. Otherwise enter 0.0. For internal gas phase print out, enter the number of the vertical plane desired (enter 1.0 for north wall plane, 6.0 for center plane, and 11.0 for south wall plane. Interpolate for planes in between).

Example Input

An example input was selected to be WOGA study tank EXXON 410 which was case study "B" since it involved flashing, working and breathing phenomena.

The following cards are:

CARD

1	Exxon 410			Base Case B				
2	30.	24.						
3	1.							
4	1.	11.	11.					
5	14.9	.86	.86					
6	1.	11.	4.	1.				
7	11.	.6						
8	18.	0.	19.	.3	18.	.6	19.	.9
8	18.	1.2	19.	1.5	18.	1.8	19.	2.1
8	18.	2.4	19.	2.7	18.	3.0		
9	170.	49.7	160.					

10	384.							
11	1.							
12	.0122	.0	.0085	.0	.0185	.0105	.0215	.014
12	.0125	.0065	.014	.0245	.0125	.027	.0028	.0
12	.0	.0009	.0					
13	9636.							
14	.157							
15	.0001							
16	.0	.02						
17	.8	.9						
18	.8	.9						
19	100.	100.	100.	100.	100.			
20	34.	199.	85.	12.				
21	80.							
22	50.							
23	.7							
24	5.							
25	25.	6.						

Section 3 initializes all the variable values necessary for entry into Section 5 the MAIN TIME section.

Section 4 is the FLASH section where a high pressure crude oil feed will be adiabatically flashed. The adiabatical flash algorithm or method was explained in the Flashing section discussion on page 23.

In addition to any possible crude feed flashing, this section also calculates the bubble point pressure of the entire crude feed with water (if present) at the temperature of the feed stock. The bubble point pressure is

the lowest pressure that the entire crude/water feed will exist as total liquid. System pressures less than the bubble point pressure will cause vapor to generate, resulting in a two phase system. Pressure greater than the bubble point pressure will cause no evaporation of the liquid phase. If the bubble point pressure is greater than the designated feed pressure, the feed contains a vapor phase and the program calculates the amount and composition of the vapor and liquid phases before flashing of the feed. If the bubble point pressure is less than the feed pressure, then the feed is all liquid phase before any flashing might occur. If the bubble point pressure is less than ambient, the liquid crude will be all liquid even after a possible flashing, so the program does not consider a flash and bypasses the flashing section for this case. The program flashes the feed by reducing the pressure to ambient conditions as specified by the user. The program assumes the temperature of the feed until the energy of the crude at the post-flash condition equals the crude energy before the flashing occurred (pre-flash condition).

After any possible flashing of the crude oil feed has occurred, the bulk liquid temperature of the tank basin liquid is established. If the bulk liquid basin temperature was specified during input, then the basin temperature will be the value read. If the basin temperature was not specified and the crude oil was not flashed, the basin temperature is set to the value of the crude feed temperature. If the basin temperature was not specified and the crude oil was flashed, then the basin temperature is set to the post-flash temperature as calculated by the program.

Section 5 is the MAIN TIME block of the program. In this section velocities, composition, and temperatures in the gas space are calculated

together with emissions throughout the entire simulated time. Section 5 is broken down into five subsections which are : Section 5A TIME RESET, Section 5B GAS VELOCITIES, Section 5C GAS COMPOSITION, Section 5D EMISSIONS and Section 5E GAS TEMPERATURES.

The TIME RESET Section (Section 5A) is responsible for continually updating the values of all variables that change with time. Included in this section are the clearness index (CLEAR), daily high temperature (TAH), daily low temperatures (TAL), wind velocity (VWIND), exact time of day (EXTIME), gas space density at each calculated point (RHO), tank pressure (P), outage (H), vertical velocity of the liquid surface (DHDT), and rate of change of gas volume due to temperature and pressure changes (DVDT).

The GAS VELOCITIES section (Section 5B) calculates the gas velocities in the horizontal x direction, V_x , the horizontal y direction, V_y , and in the vertical z direction, V_z , at each point in the gas space. Momentum Equations (1), (2), (3) and (4) are solved in this section.

In the GAS COMPOSITION section (Section 5C) the concentrations of all species are calculated at each point in the gas space. Compositions are calculated by Equation (5) with Equations (6) and (7). Equation (9), (10), and (12) are also used in this section to establish the species concentrations at the gas/liquid interface.

The hydrocarbon emissions are calculated in the EMISSIONS section (Section 5D). The amount of each species that emits from the dome vent during exhale is calculated by Equation (8). The exiting gas composition and gas volume emitted are also obtained.

The temperatures of the gas at every point in the gas space are calculated in Section 5E (GAS TEMPERATURES). The gas temperatures are calculated from Equation (13). Equations (14), (15), (16), (17), (18),

(19), (20), (21), and (22) are used to establish the dome metal, wall metal and liquid surface temperatures, which aids in the solution of Equation (13).

Section 6 FUNCTION VLE uses quadratic polynomial interpolation to calculate the vapor/liquid equilibrium constant, K, for each species at any temperature and pressure. Section 6 is used mainly by Section 4 to assess crude feed flashing where equilibrium values are needed at pressures greater than atmospheric pressure.

REFERENCES

- API Bulletin 2512, 1957.
- API Bulletin 2513, 1959.
- API Bulletin 2518, 1962.
- AP-42 Supplement 12, 1981.
- Beckman, J. R., IASTED, ACTA Press, 1983.
- Beckman, J. R., I&EC Des. Dev., 23, 472, 1984.
- Beckman, J. R. and J. R. Gilmer, I&EC Des. Dev. 20 (646), 1981.
- Beckman, J. R. and J. A. Holcomb, I&EC Des. Dev. January 1986.
- Browne, L. W. B., Numerical Simulation of Fluid Motion, ed. John Noye, p. 223, 1978.
- DePriester, C.L., Chem Eng. Progr., Symposium Ser. 7:49 (1953).
- Duffie, J. A., W.A. Beckman, Solar Engineering of Thermal Processes, John Wiley, 1980.
- Edmister, Lee, Applied Hydrocarbon Thermodynamics, 1983.
- Engineering-Science Inc., Arcadia, CA, 1977.
- Guistra, D. P., MS Thesis, Arizona State University, 1983.

Holcomb, J. A., MS Thesis, Arizona State University, 1983.

Incropera, F. P., D. P. Dewitt, Fundamentals of Heat Transfer, John Wiley,
1981.

Sahakian, J. A., MS Thesis, Arizona State University, 1983.

Vrentas, J. S. and J. L. Duda, Appl. Sci. Res. 28, p. 241, 1973.

Glossary of Terms

ao	coefficient
a1	coefficient
C(gas)	total concentration in gas phase, lb moles/ft ³
Ci	gas phase concentration of species i, lb moles/ft ³
Ci (bulk liq)	liquid concentration of species i bulk, lb moles/ft ³
Ci (gas sur)	gas concentration of species i at liquid surface, lb moles/ft ³
Ci (liq boil)	concentration of species i in liquid at boiling, lb moles/ft ³
Ci (liq sur)	liquid concentration of species i at surface, lb moles/ft ³
C liq	total liquid phase concentration, lb moles/ft ³
Cp	gas phase heat capacity, BTU/lb mole °F
d	pertain to dome
del	earth's angle of declination, degrees
Dil	liquid phase diffusivity of species i, ft ² /hr
Dim	gas phase diffusivity of species i, ft ² /hr
Edo	emissivity of dome outside surface
E _{di}	emissivity of dome inside surface
E _i	emissions flux of species i, lb moles/ft ²
E1	emissivity of dome inside
E2	emissivity of wall inside
E3	emissivity of liquid surface
F _{hc}	hydrocarbon feed rate, lbmoles/hr
film	thickness of liquid surface resistance layers ft
F _w	water feed rate, lbmoles/hr
F12	view factor dome to wall
F13	view factor dome to liquid

F21	view factor wall to dome
F23	view factor wall to liquid
F31	view factor liquid to dome
F32	view factor liquid to wall
g	acceleration of gravity, ft/hr^2
Gamma	angle to meridian from surface, degrees
G1	$= \sigma T_d^4 i$, $\text{BTU/ft}^2\text{hr}$
G2	$= \sigma T_w^4 i$, $\text{BTU/ft}^2\text{hr}$
G3	$= \sigma T_l^4$, $\text{BTU/ft}^2\text{hr}$
H	outage height, ft
i	species i
I	Planar continuity integral, ft^3/hr
Ib	total beam radiation, $\text{BTU/ft}^2\text{hr}$
Iclear	clearness ratio
Id	diffuse radiation, $\text{BTU/ft}^2\text{hr}$
IdI	diffuse fraction of total radiation
Ihor	total radiation on a horizontal surface, $\text{BTU/ft}^2\text{hr}$
Io	hourly extraterrestrial horizontal radiation, $\text{BTU/ft}^2\text{hr}$
Ivert	total solar flux to a vertical wall, $\text{BTU/ft}^2\text{hr}$
J1	radiosity of dome, $\text{BTU/ft}^2\text{hr}$
J2	radiosity of wall, $\text{BTU/ft}^2\text{hr}$
J3	radiosity of liquid surface, $\text{BTU/ft}^2\text{hr}$
k	gas phase thermal conductivity, $\text{BTU/ft hr } ^\circ\text{F}$
K	vapor/liquid equilibrium constant
Kd	dome metal thermal conductivity $\text{BTU/ft hr } ^\circ\text{F}$
Kg	thermal conductivity of gas, $\text{BTU/ft hr } ^\circ\text{F}$
Ki	vapor/liquid equilibrium constant for species i

Kl liquid phase thermal conductivity, BTU/ft hr °F
 Ld dome metal thickness, ft
 Li dome insulation thickness, ft
 Mb molecular weight of liquid mixture, lb/lb mole
 N number of day light hours, hrs
 Nday day of year
 Ni molar flux of species i in gas phase, lb moles/ft² hr
 P_{hc} pressure of hydrocarbon, psia
 Phi latitude, degree
 P_{total} total pressure, psia
 P_w Pressure of water, psia
 Q_{conv} dome convection energy flux to ambient, BTU/ft²hr
 Q_{dome} dome conduction energy flux, BTU/ft²hr
 Q_{hc} quality of hydrocarbon (vapor fraction)
 Q_{rad1} radiation flux from dome, BTU/ft²hr
 Q_{rad2} radiation flux from wall, BTU/ft²hr
 Q_{rad3} radiation flux from liquid, BTU/ft²hr
 Q_{sky} energy flux reradiated to sky, BTU/ft²hr
 Q_{solar} incident solar radiation flux, BTU/ft²hr
 Q_w quality of water (vapor fraction)
 R tank radius, ft
 t time, hrs
 T liquid temperature, °F
 T_{air} air temperature, °F
 T_b beam radiation, BTU/ft²hr
 T_d diffuse radiation, BTU/ft²hr
 T_{dawn} time of dawn, hr

Tdi	dome inside temperature, °F
Tdo	dome outside temperature, °F
Tgas	gas phase temperature, °F
Time	time, hr
Tl	liquid surface temperature, °F
Tset	time of sun set, hr
U	ambient heat transfer coefficient, BTU/ft ² hr °F
Vx	gas velocity in horizontal north/south direction, ft/hr
Vy	gas velocity in horizontal east/west direction, ft/hr
Vz	gas velocity in vertical direction, ft/hr
w	pertains to wall
W	solar angle, degrees
Ws	sunset angle, degrees
X	horizontal north/south direction, ft
X(i)	mole fraction in liquid
y	horizontal east/west direction, ft
Y(i)	mole fraction in vapor
z	vertical direction, ft
Z(i)	mole fraction in feed composite
<u>Greek</u>	
λ	heat of vaporization BTU/lb mole
μ	gas viscosity lb/ft hr
ρ	gas density lb/ft ³
$\bar{\rho}$	average gas density on horizontal phase lb/ft ³
σ	stephan - Boltzmann constant
θ	angle of incidence to a surface, degrees
θz	angle of beam incidence to horizontal, degrees

Acronyms

API	American Petroleum Institute
ARB	California Air Resources Board
CPU	Central Processing Unit
EPA	Environment Protection Agency
LACT	Lease Automatic Custody Transfer
WOGA	Western Oil and Gas Association

Computer DATA Variables

Section 1

ALPH	Thermal conductivity/heat capacity. lbmoles/ft. hr.
CPA	Liquid heat capacity constant in $C_p = C_{pA} + C_{pB}^* (T-100)$
CPB	Liquid head capacity constant in $C_p = C_{pA} + C_{pB}^* (T-100)$
CPDI	Heat capacity of dome insulation, BTU/lb°F
CPDM	Heat capacity of dome metal, BTU/lb°F
CPWI	Heat capacity of wall insulation, BTU/lb°F
CPWM	Heat capacity of wall metal, BTU/lb°F
DIFFO	Gas phase hydrocarbon diffusivity, ft ² /hr
DIFLO	Liquid phase hydrocarbon diffusivity, ft ² /hr
DELHO	Hydrocarbon heat of vaporization, BTU/lbmole
GAM	Angles between exact south and any point on tank
KDI	Thermal conductivity of dome insulation, BTU/ft hr°F
KDM	Thermal conductivity of dome metal, BTU/ft hr°F
KWI	Thermal conductivity of wall insulation, BTU/ft hr°F
KWM	Thermal conductivity of wall metal, BTU/ft hr°F
MW	Hydrocarbon molecular weight

RHODI	Density of dome insulation, lb/ft ³
RHODM	Density of dome metal, lb/ft ³
RHOWI	Density of wall insulation, lb/ft ³
RHOWM	Density of wall metal, lb/ft ³
TB	Hydrocarbon normal boiling point, °F
TC	Hydrocarbon critical point, °F
TDM	Thickness of dome metal, ft
TWM	Thickness of wall metal, ft
XKVLE	Vapor/liquid equilibrium constant
XNAM1	First half of hydrocarbon names
XNAM2	Second half of hydrocarbon names
XP	Pressure of data K values, psia
XT	Temperature of data K values, °F

Computer READ Variables (Section 2)

ALT	Altitude above sea level, ft
AMBP	Ambient pressure, psia
BULK	Temperature of tank basin, °F
CLEA	Solar clearness index
CLIQ	Liquid density at 60°F, lbmoles/ft ³
CYCLE	Length of a cycle, hours
D	Tank diameter, ft
DAY	Day of this year
DV	Vent diameter, ft
DVF	Post-flash vent diameter, ft
EDI	Inside dome emissivity
EDO	Outside dome emissivity
EWI	Inside wall emissivity
EWO	Outside wall emissivity
FHC	Hydrocarbon feed rate
FHI	Latitude, degrees
FILM	Liquid film resistance thickness, ft
FW	Total water feed rate, BBls/day
HLIQ	Outage, ft
HT	Tank height, ft
PF	Feed pressure, psia
PRESH	Vent pressure setting, inches of water
PRESL	Vent vacuum setting, inches of water
T1DAY	Time of day for cycle start, hours
TDI	Dome insulation thickness, ft

TF	Feed temperature, °F
TINIT	Initial tank gas temperature, °F
TLIQ	Time at an outage, hours
TTAH	Daily high temperature, °F
TTAL	Daily low temperature, °F
TWI	Wall insulation thickness, ft
VWIN	Wind velocity, MPH
XCOMP	Composition print index
XDATA	Number of outage data sets
XMF	Hydrocarbon feed composition index
XSET	Composition vertical plane print index
XV	Vent location in X direction
XVENT	Number of emitting dome vents
YV	Vent location in y direction
Z	Feed composition
ZV	Vent location in z direction

Section 3 Variables

CA	Gas phase species concentration, lbmoles/ft ³
DELT	Time step, hours
DELX	Distance step, ft
EL	Emissivity of liquid surface, 0.95
IFLAS	x location of vapor post-flash vent
II	Total number of points in x direction, 21
JFLAS	y location of vapor post-flash vent
JJ	Total number of points in y direction, 21

J1	West wall location index in y direction
J2	East wall location index in y direction
KK	Liquid surface z direction index
KL	Thermal conductivity of liquid, 0.08 BTU/ft hr°F
PHI	Dimensionless concentration
RADF	Radiation convergence coefficient, 0.1
TG	Gas phase temperature, °F
TSET	Time of sunset, hours
TDAWN	Time of sunrise, hours
VLEK	Vapor/liquid equilibrium constant

Computer Section 4 Variables

ALPHA	Thermal diffusivity, ft ² /hr
KG	Thermal conductivity of gas, BTU/ft hr°F
P	Tank pressure, psia
PBUB	Bubble point pressure of feed, psia
PHC	Vapor pressure of hydrocarbon, psia
PW	Vapor pressure of water, psia
QHC	Hydrocarbon quality (fraction vaporized)
QW	Water quality (fraction vaporized)
X	Mole fraction in liquid phase
Y	Mole fraction in vapor phase
Z	Mole fraction in feed

Computer Section 5A Variables

CLEAR	Solar clearness index
DVDT	Rate of change of gas volume due to
EMISS1	Total emissions, lbs
EMISS2	Propane plus emissions, lbs
EXTIM	Exact time, hours
ISTOP	Stopping time index
ITIME	Time index
RHO	Gas density, lbs/ft ³
TAH	Daily high temperature, °F
TAL	Daily low temperature, °F
TGA	Average gas phase temperature, °F
UD	Dome heat transfer coefficient, BTU/ft ² hr°F
UW	Wall heat transfer coefficient, BTU/ft ² hr°F
VEMIT	Total standard gas volume emitted, ft ³
VIN	Total standard gas volume enhaled, ft ³
VWIND	Wind velocity, MPH

Computer Section 5B Variables

DHDT	Rate of change of liquid surface position, ft/hr
H	Outage, ft
VOLV	Total gas volume rate of change, ft ³ /hr
VX	Gas velocity in horizontal x direction, ft/hr
VY	Gas velocity in horizontal y direction, ft/hr
VZ	Gas velocity in vertical z direction, ft/hr

Computer Section 5C Variables

CA	Gas phase species concentration, lbmoles/ft ³
CASUR	Liquid phase species concentration at the liquid surface, lb moles/ft ³
NA	Species molar flux at the liquid surface lbmoles/ft ² hr
VSTAR	Total gas velocity at the liquid surface, ft/hr

Computer Section 5D Variables

EMISS1	Total emission, lbs
EMISS2	Propane plus emissions, lbs
EPPH1	Rate of total emissions, lb/hr
EPPH2	Rate of propane plus emissions, lb/hr
GASV	Vent gas rate at 60°F, ft ³ /min
X1	Species mole fraction in vent gas based on total emissions
X2	Species mass fraction in vent gas based on total emissions
X3	Species mole fraction in vent gas based on propane plus emissions
X4	Species mass fraction in vent gas based on propane plus emissions

Computer Section 5E Variables

F12	Radiation view factor from dome to wall
F13	Radiation view factor from dome to liquid
F21	Radiation view factor from wall to dome
F23	Radiation view factor from wall to liquid
F31	Radiation view factor from liquid to dome

F32	Radiation view factor from liquid to wall
IB	Total beam radiation, $\text{BTU}/\text{ft}^2 \text{ hr}$
ID	Diffuse radiation, $\text{BTU}/\text{ft}^2 \text{ hr}$
ITOT	Total incident radiation, $\text{BTU}/\text{ft}^2 \text{ hr}$
JD	Interval dome radiosoty, $\text{BTU}/\text{ft}^2 \text{ hr}$
JL	Internal liquid radiosoty, $\text{BTU}/\text{ft}^2 \text{ hr}$
JW	Internal wall radiosoty, $\text{BTU}/\text{ft}^2 \text{ hr}$
QSOLD	Total external dome incident radiation, $\text{BTU}/\text{ft}^2 \text{ hr}$
QSOLE	Total external incident radiation on the eastern wall, $\text{BTU}/\text{ft}^2 \text{ hr}$
QSOLW	Total external incident radiation on the western wall, $\text{BTU}/\text{ft}^2 \text{ hr}$
RADD	Net internal dome radiation, $\text{BTU}/\text{ft}^2 \text{ hr}$
RADL	Net internal liquid radiation, $\text{BTU}/\text{ft}^2 \text{ hr}$
RADW	Net internal wall radiation, $\text{BTU}/\text{ft}^2 \text{ hr}$
TA	Ambient temperature, °F
TAUB	Beam radiation, $\text{BTU}/\text{ft}^2 \text{ hr}$
TAUD	Diffuse radiation, $\text{BTU}/\text{ft}^2 \text{ hr}$
TDO	Dome outside temperature, °F
TG	Gas temperature, °F
TWO	Wall outside temperature, °F
W	Solar angle, degrees

Computer Section 6 Variables

P	Hydrocarbon pressure, psia
T	Temperature, °F
VLE	Vapor/liquid equilibrium constant
XO	Pressure of data K values, psia
XT	Temperature of data K values, °F

APPENDIX


```

166. 22 CONTINUE
167.  CARD #5 AMBIENT PRESSURE(PRESI),PRESSURE AND VACUUM SETTINGS(IN WATER)
168.  READ(NR,21)AMBPP,PRESH,PRESL
169.  C      IF ZEROS ARE READ FOR THESE VARIABLES, THEN THE
170.  C      DEFAULT VALUES ARE
171.  C      IF(CAMBPP.EQ.0.) AMBP=14.7
172.  C      IF(CPRESH.EQ.0.) PRESH=0.
173.  C      IF(CPRESL.EQ.0.) PRESL=0.
174.  C      WRITE(NH,26)AMBPP,PRESH,PRESL
175.  C      PRESH=14.7+PRESH/26.
176.  C      PRESL=14.7+PRESL/26.
177.  C      SIZE AND LOCATION OF VAPOR POST-FLASH VENT
178.  C      READ(NR,21)DVV,XV,YV,ZV
179.  C      DEFAULT CARD: S ARE
180.  C      IF(CXV.EQ.0.) XV=11.
181.  C      IF(CYV.EQ.0.) YV=11.
182.  C      IF(CZV.EQ.0.) ZV=1.
183.  C      IF(CV.V.EQ.0.) DVV,XV,YV,ZV
184.  C      WRITE(NH,26)DVV,XV,YV,ZV
185.  C      IF(CV.V.EQ.0.) DVV,XV,YV,ZV
186.  C      DFLAS=DVF
187.  C      IFLAS=XV+.1
188.  C      JFLAS=YV+.1
189.  C      KFLAS=ZV+.1
190.  C      AF=3.14*(COVF**2)/4.
191.  C      LIQUID SURFACE LOCATION(OUTAGE) VERSUS TIME(HRS) DATA
192.  C      READ(NR,21)XDATA,CYCLE
193.  C      NUMBER OF DATA SETS AND HOURS PER CYCLE
194.  C      DEFAULT CARD: S ARE
195.  C      IF(CXDATA.EQ.0.) XDATA=2.
196.  C      IF(CYDATA.EQ.0.) CYCLE=24.
197.  C      IF(CCYCLE.EQ.0.) CYCLE=24.
198.  C      NDATA=XDATA+.1
199.  C      WRITE(NH,26)XDATA,CYCLE
200.  C      IF(CCYCLE.LT.001)CYCLE=24.
201.  C      LIQUID OUTAGE(FEET) WITH TIME(HRS)
202.  C      READ(NR,21)(HLIQ(I),TLIQ(I),I=1,NDATA)
203.  C      DEFAULT CARD: S ARE
204.  C      IF(CCYCLE.LT.001)CYCLE=24.
205.  C      LIQUID OUTAGE(FEET) WITH TIME(HRS)
206.  C      READ(NR,21)(HLIQ(I),TLIQ(I),I=1,NDATA)
207.  C      DEFAULT CARD: S ARE
208.  C      IF(CCYCLE.LT.001)CYCLE=24.
209.  C      LIQUID OUTAGE(FEET) WITH TIME(HRS)
210.  C      READ(NR,21)(HLIQ(I),TLIQ(I),I=1,NDATA)
211.  C      LIQUID TEMPERATURE(F), PRESSURE(PRESI),TANK LIQUID
212.  C      TEMPERATURE(IF HEATED)(F)
213.  C      READ(NR,21)TF,PF,BULK
214.  C      DEFAULT CARD: S ARE
215.  C      IF(CTF.EQ.0.) TF=150.
216.  C      IF(CPF.EQ.0.) PF=14.7
217.  C      WRITE(NH,26)TF,PF,BULK
218.  C      TOTAL WATER FLOW RATE(BBLS/DAY)
219.  C      READ(NR,21)FW

```

```

221. WRITE(CNR,26) FW FRACTION ENTER 1 ; IF MASS FRACTION ENTER 2
222. IF MOLE FRACTION ENTER 1 ; IF MASS FRACTION ENTER 2
223. AD(CNR,21)XMF
224. MF=XMF+.1
225. WRITE(CNR,26)XMF
226. #12(CNR,21)XMF SPECIES FRACTION IN FEED(WATER FREE BASIS)
227. READ(CNR,21)(ZC(I),I=1,LEND)
228. WRITE(CNR,26)(ZC(L),L=1,LEND)
229. FORMAT(5X,8C(2X,F10.5))
230. #26(CNR,21)TOTAL HYDROCARBON PLUS DISSOLVED GASES IN FEED((8BLS/DAY)NO WATER)
231. READ(CNR,21)FHC
232. DEFAULT CARD. IF ZEROS ARE READ FOR THESE VARIABLES, THEN THE
233. DEFAULT VALUES ARE :
234. FHC=100.
235. WRITE(CNR,26) FHC
236. #14(CNR,21) LIQUID DENSITY(LBMOLES/CU FT)
237. READ(CNR,21) CLIQ
238. DEFAULT CARD. IF ZEROS ARE READ FOR THESE VARIABLES, THEN THE
239. DEFAULT VALUES ARE :
240. CLIQ=.3
241. WRITE(CNR,26) CLIQ
242. #15(CNR,21) LIQUID FILM RESISTANCE THICKNESS(FEET)
243. READ(CNR,21) FILM
244. WRITE(CNR,110) FILM
245. FILMH=FILM
246. #16(CNR,21) DGME AND WALL INSULATION THICKNESS(FT)
247. READ(CNR,21)TDI,TDI,TDI
248. WRITE(CNR,26)TDI,TDI,TDI
249. #17(CNR,21) DGME OUTSIDE AND INSIDE EMISSIVITY
250. READ(CNR,21)E0,E0,E0
251. DEFAULT CARD. IF ZEROS ARE READ FOR THESE VARIABLES, THEN THE
252. DEFAULT VALUES ARE :
253. E0=.9
254. E0=.9
255. E0=.9
256. WRITE(CNR,26)E0,E0,E0
257. #18(CNR,21) WALL OUTSIDE AND INSIDE EMISSIVITY
258. READ(CNR,21)E0,E0,E0
259. DEFAULT CARD. IF ZEROS ARE READ FOR THESE VARIABLES, THEN THE
260. DEFAULT VALUES ARE :
261. E0=.9
262. E0=.9
263. E0=.9
264. WRITE(CNR,26)E0,E0,E0
265. #19(CNR,21) INITIAL TANK GAS TEMPERATURE(F) TOP TO LIQUID SURFACE
266. READ(CNR,21)T(I),I=1,5)
267. DEFAULT CARD. IF ZEROS ARE READ FOR THESE VARIABLES, THEN THE
268. DEFAULT VALUES ARE :
269. T(I)=100.
270. T(I)=100.
271. T(I)=100.
272. T(I)=100.
273. T(I)=1,5)
274. WRITE(CNR,110)(TIMEES),ALTITUDE (FT), DAY OF YEAR, TIME OF
275. #20(CNR,21) LATITUDE (DEGREES), 24 HR CLOCK

```


331.
332.
333.
334.
335.
336.
337.
338.
339.
340.
341.
342.
343.
344.
345.
346.
347.
348.
349.
350.
351.
352.
353.
354.
355.
356.
357.
358.
359.
360.
361.
362.
363.
364.
365.
366.
367.
368.
369.
370.
371.
372.
373.
374.
375.
376.
377.
378.
379.
380.
381.
382.
383.
384.
385.

C INTO SECTION 5 THE MAIN TIME SECTION.
C ENTRY .6Y..1) Z(I9)=1.
C DEW POINT TEMPERATURE
C TOP=50.
C FW=42.*8.34/(24.*118.)
C FFHC=42.*CLIQ/(24.*7.48)
C IFP(MF.NE.2)GO TO 569
C CONVERT ALL FEED COMPOSITIONS TO MOLE FRACTIONS
C DO 570 L=1,LEND
C Z(L)=Z(L)/MW(L)
C SUM=SUM+Z(L)
C DO 571 L=1,LEND
C Z(L)=Z(L)/SUM
C CONTINUE
C DO 622 L=1,20
C DR(L)=(DIFFO(L)-DIFFO(1))/(DIFFO(12)-DIFFO(1))
C DO 20 L=1,LEND
C XT12=XT(2)-XT(1)
C AK(L)=XKVL(1,1,L)
C BK(L)=(XKVL(2,1,L)-AK(L))/XT12
C CK(L)=(XKVL(3,1,L)-2.*XKVL(2,1,L)+AK(L))/(2.*XT12+XT12)
C EXTIME=1DAY
C DEL=23.45*INC(2.*3.14*(284.+DAY)/365.)
C SDEL=SIN(3.14*DEL/180.)
C COSL=COS(3.14*DEL/180.)
C SPHI=SPIN(3.14*FHI/180.)
C DEW=C(8.+TDP/450.)*.25
C T00=560.
C DO 2 I=1,21
C TWDE(I)=T00
C TWOW(I)=T00
C 2 STEPHAN-BOLTZMAN CONSTANT
C SIG=.173E-8
C SEMISSIVITY OF LIQUID SURFACE
C EMISS=.95
C THERMAL CONDUCTIVITY OF LIQUID PHASE
C KL=.08
C RADIATION CONVERGENCE COEFFICIENT(SELECT BETWEEN 0.0 AND 1.0)
C RADF=.1
C SLRCD=TO*RRHODM*CPDM+TO*RRHODI*CPDI
C SLRCW=TW*RRHOWM*CPWM+TW*RRHOWI*CPWI
C SLFKD=TO/KOM
C IF(KDI.GT.0.) SLKD=SLKD+TOI/KOI
C SLKW=TW/KWM
C IF(KWI.GT.0.) SLKW=SLKW+TWI/KWI
C SET DELTA TIME
C DELT=1.
C NMI=NDATA-1
C IIM1=21
C IIM2=IIM1-1
C R=D/2.
C SET DELTA DISTANCE
C DELX=D/(IIM1-1)

```

386. DO 573 I=1,NM1
387. IP1=I+1
388. SLOPE=ABS((HLIQ(IP1)-HLIQ(I))/(TLIQ(IP1)-TLIQ(I)))
389. IF (SLOPE.LT..001) GO TO 573
390. DELTT=DELX/SLOPE
391. IF(DELTT.GT. DELTT) DELT=DELTT
392. DELTT=.5*(TLIQ(IP1)-TLIQ(I))
393. IF(DELTT.GT. DELTT) DELT=DELTT
394. CONTINUE
395. ICYC=CIRCLE/DELX
396. KK=HLIQ(1)/DELX+1.1
397. KKM1=KK-1
398. KKM2=KK-2
399. JJ=I
400. IIV=(I-1)/2+1
401. JVV=IIV
402. IIVM1=IIV-1
403. IIVP1=IIV+1
404. DO 25 I=1,NVENT
405. IVENT(I)=(CIVENT(I)-1)/2+1
406. JVVENT(I)=(JVENT(I)-1)/2+1
407. JF=(JFLAS-1)/2+1
408. JF=(JFLAS-1)/2+1
409. A0=DELTT/(4.*DELX*DELX)
410. A2=DELTT/(2.*DELX)
411. A3=A2*2.
412. JC=IY/2. +1
413. IC=JC
414. J1(CIC)=I
415. J2(CIC)=I
416. YCM1=IC-1
417. SET EI=2,ICM1
418. DO 5 I=2,ICM1
419. XX=R-(I-1)*DELX
420. YBE=YBE/DELX
421. IN=YBE/DELX
422. DIST1=ABS(YBE-IN*DELX)
423. DIST2=ABS(YBE-(IN+1)*DELX)
424. IF(DIST2.LT. DIST1) IN=IN+1
425. IF(CI.EQ.2) IN=5
426. FORMAT(5X,F10.3,I3,I3)
427. J1(CI)=IC-IN
428. J2(CI)=IC+IN
429. J1(CI+1-I)=J1(I)
430. J2(CI+1-I)=J2(I)
431. J1(CI)=J1(C2)
432. J2(CI)=J2(C2)
433. J1(CI)=J1(IIM1)
434. J2(CI)=J2(IIM1)
435. IVC=IC/2+1
436. JVC=JC/2+1
437. DO 4 I=1,I;2
438. I=(I-1)/2+1
439. J1(IV)=(J1(I)-1)/2+1
440. J2(IV)=IIV+1-JV1(IV)

```

573

25

6

5

4

C WND WEST BOUNDARY POINTS FOR TANK WALLS

441.
442.
443.
444.
445.
446.
447.
448.
449.
450.
451.
452.
453.
454.
455.
456.
457.
458.
459.
460.
461.
462.
463.
464.
465.
466.
467.
468.
469.
470.
471.
472.
473.
474.
475.
476.
477.
478.
479.
480.
481.
482.
483.
484.
485.
486.
487.
488.
489.
490.
491.
492.
493.
494.
495.

```
DO 11 IV=1, IIV  
IF(JIV).EQ.1) GO TO 12  
CONTINUE  
IV2=IIV+1-IV1  
DO 10 K=1, KK  
DO 10 I=1, II  
J1I=J1(I)  
J2I=J2(I)  
DO 10 J=J1I, J2I  
VX(I, J, K)=0.  
VY(I, J, K)=0.  
VZ(I, J, K)=0.  
CONTINUE
```

SECTION 4 FLASH

```
SECTION 4 FLASH  
IS THE FLASH SECTION WHERE A HIGH PRESSURE CRUDE FEED TO ANY  
WILL BE ADIABATICALLY FLASHED TO TANK ALSO. CALCULATES THE BUBBLE POINT  
CRUDE FEED AT THE FLASH SECTION. AFTER ANY POSSIBLE FLASH-  
ING OF THE CRUDE HAS OCCURED, THE BULK LIQUID TEMPERATURE OF THE  
TANK BASIN LIQUID IS ESTABLISHED. IF THE BULK LIQUID TEMPERATURE  
ATURE VALUE READ, IF THE BASIN TEMPERATURE AND THE  
CRUDE FEED WAS NOT FLASHED, THEN THE BASIN TEMPERATURE IS SET TO  
THE VALUE OF THE CRUDE FEED TEMPERATURE. IF THE BASIN TEMPERATURE  
TEMPERATURE IS SPECIFIED AND THE CRUDE FEED TEMPERATURE IS SET TO  
THE PROGRAM.  
FEED ALPHA=.0023
```

THERMAL CONDUCTIVITY

```
AIR=.02  
KG=.13  
DO 13 X(L)=Z(L)  
PTEST=P  
BUBBLE POINT PRESSURE CALCULATION  
DO 306 I=1, I1  
PBUB=0.  
IF(FW.GT.1.) PBUB=EXP(15.8088-8817.3/(CT+460.))  
DO 308 L=1, 18  
PBUB=PBUB+PTEST*Z(L)*VLE(T, PTEST, L, XKVLE, XT, XP)  
WRITE(CNM, 307) PBUB  
CONTINUE  
FORMAT(5X, 'FEED BUBBLE POINT PRESSURE IS ', F10.2, ' PSIA')  
IF(PBUB.LT.AMBP) Z(18)=1.  
IF(PBUB.LT.AMBP) GO TO 14  
IF(PF.LT.15.) GO TO 14
```

```

496. FLASHING CALCULATION
497. GUESS POST-FLASH TEMPERATURE
498. DO 310 LTEMP
499. T=TF+1-LTEMP
500. PW=EXP(15.8088-8817.3/(T+460.))
501. PHC=PW-LTEMP
502. IF(CP.LT.PBUB) GO TO 309
503. QHC=0.
504. QW=0.
505. GO TO 313
506. QHC=.5
507. DO 311 LQHC=1,100
508. SUM=0.
509. ZPLUS=.1.
510. CALCULATE POST-FLASH LIQUID COMPOSITION
511. DO 312 L=1,18
512. DENOM=QHC*(VLE(T,P,L,XKVLE,XT,XP)-1.)+1.
513. IF(CABS(DENOM).LT.1.E-30) GO TO 311
514. X(L)=Z(L)/DENOM
515. ZPLUS=ZPLUS-Z(L)
516. SUM=SUMF+X(L)*(VLE(T,P,L,XKVLE,XT,XP)-1.)/DENOM
517. IF(CZPLUS.LT.0.) ZPLUS=0.
518. SUM=SUM-1.+ZPLUS/(1.-QHC)
519. QHC=QHC-SUM/(ZPLUS/(1.-QHC)+2-SUMF)
520. IF(QHC.LT.0.) OR(QHC.GT.1.) GO TO 310
521. IF(CABS(SUM).LT..01) GO TO 313
522. CONTINUE
523. CALCULATE POST-FLASH VAPOR COMPOSITION
524. DO 314 L=1,18
525. ZZ=VLE(T,P,L,XKVLE,XT,XP)
526. HVAP=0.
527. CALCULATE ENERGY OF VAPOR/LIQUID COMPOSITE
528. DO 315 L=1,18
529. CPLT=CP(L)*L*(T-TF)
530. HVAP=HVAP+Y(L)*CPLT
531. HL=HL+X(L)*CPLT
532. QW=0.
533. CALCULATE ENERGY OF VAPOR/LIQUID COMPOSITE
534. DO 315 L=1,18
535. CPLT=CP(L)*L*(T-TF)
536. HVAP=HVAP+Y(L)*CPLT
537. HL=HL+X(L)*CPLT
538. QW=0.
539. IF(CFM.GT.1.) QW=QHC*FHC*PW/(PHC*FM)
540. HTOT=FM*HHC+FM*(18.*(T-TF)+QW*DELH(T))
541. IF(HTEMP.EQ.1) WRITE(CNM,28) QHC,QW
542. FORMAT(5X,'PREFLASH QUALITY',5X,'QHC = ',F10.5,' QW = ',F10.5)
543. IF(HTEMP.EQ.1) HFEED=HTOT
544. IF(HTEMP.EQ.1) GO TO 310
545. TEST=HTOT-HFEED
546. IF(TEST)316,316,310
547. P=AMBP
548. CONTINUE
549. WRITE(CNM,29) QHC,QW,T
550.

```

```

551. 29 FORMAT(5X,'POSTFLASH QUALITY',5X,'QHC = ',F10.5,' QM = ',F10.5,
552. TEMP = ,F10.3)
553. IF(QM.GT.1.) WRITE(CM,515)
554. 515 FORMAT(5X,'ALL FEED WATER HAS EVAPORATED. PUT IN MORE WATER.STOP')
555. IF(QM.GT.1.) STOP
556. ALPHA=0.
557. 14 ALPHA=ALPHA+Y(L)*ALPHCL)
558. 7 ALPHA=CALPHA*PHC+.002*(PW)/P
559. KG=C.01*(PHC+.02*(P-PHC))/P
560. 14 PO=P
561. PRESS=PO
562. IF(QM.GT.1.) STOP
563. C=P/C.73*(T+460.)
564. TBLK=T
565. IF(BULK.GT.1.) TBLK=BULK
566. ALPHA=ALPHA/C
567. DO 321 L=1,18
568. IF(L.EQ.18.AND.KFLAS.EQ.0) GO TO 321
569. VLEK=AK(L)+BK(L)*(T-X(1))+CK(L)*(T-X(2))
570. 321 VLEK=AK(L)
571. IF(VLEK.LT.0.) VLEK=AK(L)
572. CAOB(L)=C*X(L)*VLEK
573. CONTINUE
574. C CALCULATE VAPOR PRESSURE OF HYDROCARBON LIQUID ONLY AT BULK TANK
575. LIQUID TEMPERATURE.
576. VP=0.
577. DO 588 L=1,14
578. VLEK=AK(L)+BK(L)*(TBLK-X(1))+CK(L)*(TBLK-X(2))
579. 588 IF(VLEK.LT.0.) VLEK=AK(L)
580. VP=VP+P.VLEK*X(L)
581. WRITE(CM,589)TBLK,VP
582. 589 FORMAT(5X,'LIQUID HYDROCARBON ONLY VAPOR PRESSURE AT BULK TANK ',
583. LIQUID TEMPERATURE OF ',F10.3,' F = ',F10.3,' PSIA')
584. C SET INITIAL COMPOSITION
585. DO 319 L=1,2
586. DO 319 I=1,IIV
587. DO 319 J=1,JJV
588. DO 319 K=1,KK
589. PHI(I,K)=1,KK
590. DO 1 K=1,KK
591. DO 1 I=1,IIV
592. JJV1=JVV(I)
593. JJV2=JVV(I)
594. DO 1 J=JJV1, JJV2
595. DO 1 L=1,LEND
596. CAC(I,J,K,L)=CAOB(L)
597. CONTINUE
598. DO 320 L=1,18
599. CABLK(L)=X(L)*CLIQ
600. IF(KFLAS.EQ.0) GO TO 318
601. IF(KFLAS.EQ.1) KF=1
602. IF(KFLAS.EQ.2) KF=KK
603. DO 317 L=1,18
604. CAC(I,J,K,L)=Y(L)*C*PHC/P
605.

```


661. RESECTION 5B GAS VELOCITIES, AND SECTION 5E GAS TEMPERATURES.
 662. SECTION 5C EMISSIONS, AND SECTION 5E GAS TEMPERATURES.
 663. START TIMING
 664. * * * * *
 665. * * * * *
 666. * * * * *
 667. * * * * *
 668. * * * * *
 669. * * * * *
 670. * * * * *
 671. * * * * *
 672. * * * * *
 673. * * * * *
 674. * * * * *
 675. * * * * *
 676. * * * * *
 677. * * * * *
 678. * * * * *
 679. * * * * *
 680. * * * * *
 681. * * * * *
 682. * * * * *
 683. * * * * *
 684. * * * * *
 685. * * * * *
 686. * * * * *
 687. * * * * *
 688. * * * * *
 689. * * * * *
 690. * * * * *
 691. * * * * *
 692. * * * * *
 693. * * * * *
 694. * * * * *
 695. * * * * *
 696. * * * * *
 697. * * * * *
 698. * * * * *
 699. * * * * *
 700. * * * * *
 701. * * * * *
 702. * * * * *
 703. * * * * *
 704. * * * * *
 705. * * * * *
 706. * * * * *
 707. * * * * *
 708. * * * * *
 709. * * * * *
 710. * * * * *
 711. * * * * *
 712. * * * * *
 713. * * * * *
 714. * * * * *
 715. * * * * *

SECTION 5A TIME RESET

THE TIME RESET SECTION IS RESPONSIBLE FOR CONTINUALLY UPDATING THE
 VALUES OF ALL VARIABLES THAT CHANGE WITH TIME. INCLUDED IN THIS
 SECTION ARE ALL THE CLEARANCE INDEX (TAL), DAILY HIGH TEMPERATURE (T
 AHACT), TIME OF DAY TEMPERATURE (TAL), WIND VELOCITY (VWIND),
 EXHAUSTURE AND RATE OF CHANGE OF GAS SURFACE VELOCITY (RHO), TANK
 PRESSURE AND RATE OF CHANGE OF LIQUID SURFACE VELOCITY (RHO), AND
 DENSITY SURFACE VOLUME OF GAS (DVT).
 PRESTART REMAINS IN LOOP
 DO 900 TIME=2, ISTOP
 HRS=CITIME-1, DELT
 EXTIM=EXTIM+DELT EXTIM=1.
 IF(EXTIM.GE.24) GO TO 950
 IF(EXTIM.GE.99) EXTIM, JCYC
 WFORMAT(6, 99) EXTIM, JCYC
 990 CONTINUE
 IF(EXTIM.LT.6) GO TO 582
 IBL=IBL+1
 IBL=IBL-1
 IBL=1
 DO 203 NV=1, NVENT
 WFORMAT(5X, 1) TOTAL HYDROCARBON EMISSIONS/CYCLE = , F10.2, ' LBS' /
 #F10.2, ' LBS' FOR CYCLE ', I2, ' VENT NO. ', I2)
 EMISS2(CJYC)=0.
 JCYC=CJYC+1
 CLEAR=CLEAR(CJYC)
 TAL=TAL(CJYC)
 VWIND=VWIND(CJYC)
 GO TO 581
 TAL=TAL(1)
 VWIND=VWIND(1)
 CLEAR=CLEAR(1)
 CONTINUE
 VENT=0.
 UD=1.55*(VWIND)**.6/(O*D*HT)**.133
 IF(CUD.LT..88) UD=.88
 UW=UD
 IDI=1.
 IF(CLEAR.GE..48) AND(CLEAR.LT.48) IDI=1.-1*(CLEAR
 IF(CLEAR.GE..48) AND(CLEAR.LT.1.1) IDI=1.1+.0396*(CLEAR-.789)*(CLEAR

```

716.  #) 204 C CLEAR,GE.1.1) IDI=.2
717.  IF(CONTINUE
718.  TGAO=TGA
719.  COUNT=0.
720.  TGA=0.
721.  DENSITY CALCULATION
722.  DO 60 K=1,KK
723.  RHOA(K)=0.
724.  COUNK=0.
725.  DO 58 I=1,II
726.  JJ1=J1(I)
727.  JJ2=J2(I)
728.  DO 58 J=JJ1,JJ2
729.  IV=(I-1)/2+1
730.  JV=(J-1)/2+1
731.  RHO(I,J,K)=0.
732.  DO 59 L=1,19
733.  RHO(I,J,K)=RHO(L)*CACIV,JV,K,L)*(T+460.)/(CTG(I,J,K)+460
734.  #)
735.  COUNK=COUNK+1.
736.  RHOA(K)=RHOA(K)+RHO(I,J,K)
737.  COUNT=COUNT+1.
738.  TGA=TGA+TG(I,J,K)
739.  RHOA(K)=RHOA(K)/COUNK
740.  CONTINUE
741.  TGA=TGA/COUNT
742.  IF(IITIME.EQ.2) TGAO=TGA
743.  PD=P
744.  P=PRESS
745.  GAS PHASE VOLUME CHANGE DUE TO TEMPERATURE AND PRESSURE EFFECTS
746.  DVDT=-3.14*DD*DH*(CTGA+460.)*PO/(CTGAO+460.)*P-1.)/(4.*DELTA
747.  DO 661 K=2,KKM1
748.  JJ1=J1(I)
749.  JJ2=J2(I)
750.  DO 662 J=JJ1,JJ2
751.  RHO(I,J,K)=RHO(I,J,K)
752.  RHO(I,J,K)=RHO(I,J,K)
753.  DO 661 I=1,II
754.  JJ1=J1(I)
755.  JJ2=J2(I)
756.  JPI=JJ1+1
757.  JMI=JJ2-1
758.  RHO(I,JPI,K)=RHO(I,JJ1,K)
759.  RHO(I,JMI,K)=RHO(I,JJ2,K)
760.  #)
761.  #)
762.  #)
763.  #)
764.  #)
765.  #)
766.  #)
767.  #)
768.  #)
769.  #)
770.  #)

```

SECTION 5C GAS VELOCITIES

THE GAS VELOCITIES SECTION CALCULATES THE GAS PHASE VELOCITIES IN THE HORIZONTAL (VX) AND IN THE VERTICAL (VZ) DIRECTION (VZ) AT EACH POINT IN THE GAS SPACE BY SOLVING THE MOMENTUM EQUATIONS.

```

771. DO 53 IH=1, NDATA
772. IF(CHRS.LE.FLIQ(IH))GO TO 54
773. CONTINUE
774. IHM1=IH-1
775. C CALCULATE LIQUID SURFACE VELOCITY
776. DHOT=(HLI(IH)-HLI(IHM1))/(TLI(IH)-TLI(IHM1))
777. C CALCULATE OUTAGE
778. H=HLI(IHM1)+DHOT*(CHRS-TLI(IHM1))
779. XH=H
780. KKNEW=XH/DELX+1.1
781. IF(KK.GE.KKNEW) GO TO 587
782. DO 586 IV=1, IIV
783. DO 586 JV=1, JJV
784. PHI(IV, JV, KKNEW, 1)=PHI(IV, JV, KK, 1)
785. PHI(IV, JV, KKNEW, 2)=PHI(IV, JV, KK, 2)
786. DO 586 L=1, LEND
787. IF(Z(L).LT.1.E-10) GO TO 586
788. C AC(IV, JV, KKNEW, L)=CA(IV, JV, KK, L)
789. CONTINUE
790. KK=KKNEW
791. KK1=KK-1
792. KK2=KK-2
793. IF(KF.EQ.1)VZ(IFLAS, JFLAS, KF)=VFLAS
794. SUM=0.
795. C CALCULATE COMPOSITE GAS VELOCITY AT LIQUID SURFACE
796. DO 3 I=2, IIM1
797. J1P1=J1(I)+1
798. J2M1=J2(I)-1
799. DO 3 J=J1P1, J2M1
800. VZ(I, J, KK)=DHOT+VDIFF(I, J)
801. SUM=SUM+VZ(I, J, KK)
802. VOLV=-VOLV+SUM*DELX*DELX+OVDT
803. IF(KF.EQ.2) VZ(IFLAS, JFLAS, KK)=-VFLAS
804. C ESTABLISH TANK PRESSURE
805. PRESS=PRESS-VOLV*DELTA#4./(3.14*DHOT*H)
806. IF(PRESS.GT.PRESL)PRESS=PRESL
807. IF(PRESS.LT.PRESL)PRESS=LT.PRESL
808. IF(PRESS.GT.PRESL.AND.PRESS.LT.PRESH)VOLV=0.
809. SUM=0.
810. DO 55 NV=1, NVENT
811. SUM=SUM+3.14*(OVENT(NV)**2)/4.
812. DO 56 NV=1, NVENT
813. IVE=IVENT(NV)
814. JVE=JVENT(NV)
815. VZ(IVE, JVE, 1)=VOLV/SUM
816. CONTINUE
817. IF(KFLAS.EQ.1)VOLV=VOLV+VOLF
818. IF(KFLAS.EQ.2) VZ(IFLAS, JFLAS, KK)=-VFLAS+DHOT
819. KSEE=-1
820. DO 71 KCONV=1, 4
821. KSEE=-KSEE
822. C CALCULATE VZ
823. DO 70 KI=2, KK1
824. K=KI
825. IF(VOLV.LT.0.)K=KK+1-KI

```

```

KPI=K+1
KMI=K-1
ISEE=-1
DO 74 JCONV=1,2
ISEE=-ISEE
DO 75 IX=2,IIM1
I=IX
IF(I SEE.LT.0)I=II+1-IX
J1P1=J1(I)+1
J2M1=J2(I)-1
IPI=I+1
IMI=I-1
DO 75 JX=J1P1,J2M1
J=JX
IF(I SEE.LT.0)J=J2M1+J1P1-JX
JPI=J+1
JMI=J-1
TEMPVZ=(VZ(IP1,J,K)+VZ(IM1,J,K)+VZ(JP1,K))+
#VZ(JI,J,K)+VZ(JI,J,KM1)+VZ(JI,J,KPI))
TERM=(1.4E9)*DELX*DELX*(RHO(I,J,K)-RHOA(K))
VZ(I,J,K)=VZ(I,J,K)+TERM
DELV=(VZ(I,J,KPI)-VZ(I,J,KM1))*DELX
ADENOM=ABS(DENOM)
IF(ADENOM.GT.1.)VZ(I,J,K)=VZ(I,J,K)/ADENOM
CONTINUE
SUMZ=0.
DO 76 I=1,II
JJ1=J1(I)
JJ2=J2(I)
CONTINUITY INTEGRAL CHECK
DO 76 J=JJ1,JJ2
SUMZ=SUMZ+VZ(I,J,K)
ERRER=VOLV-SUMZ*DELX*DELX
ERVZ=1.
IF(ABS(SUMZ).GT.1.)ERVZ=ABS(VOLV)/ABS(SUMZ)
DO 150 I=1,II
DO 150 J=1,JJ
VZ(I,J,K)=VZ(I,J,K)*ERVZ
CONTINUE
CONTINUE
KSEE=-1
DO 41 KCONV=1,2
KSEE=-KSEE
DO 40 KI=2,KKM1
K=KI
IF(KSEE.LT.0) K=KK+1-KI
KPI=K+1
KMI=K-1
ISEE=-1
DO 62 JCONV=1,2
I SEE=-ISEE

```

826.
827.
828.
829.
830.
831.
832.
833.
834.
835.
836.
837.
838.
839.
840.
841.
842.
843.
844.
845.
846.
847.
848.
849.
850.
851.
852.
853.
854.
855.
856.
857.
858.
859.
860.
861.
862.
863.
864.
865.
866.
867.
868.
869.
870.
871.
872.
873.
874.
875.
876.
877.
878.
879.
880.

75
74

76

150
70
71

C

C

936.
937.
938.
939.
940.
941.
942.
943.
944.
945.
946.
947.
948.
949.
950.
951.
952.
953.
954.
955.
956.
957.
958.
959.
960.
961.
962.
963.
964.
965.
966.
967.
968.
969.
970.
971.
972.
973.
974.
975.
976.
977.
978.
979.
980.
981.
982.
983.
984.
985.
986.
987.
988.
989.
990.

DO 400 L=1,2
DO 405 KX=2, KKM1
K=KX
IF(VOLV.LT.0.) K=KK+1-KX
KM1=K-1
KPI=K+1
DO 404 IV=1, IIV
DO 404 JV=1, JJV
CAO(IV, JV)=PHI(IV, JV, K, L)
CONTINUE
ISEE=-1
DO 411 ICONV=1, 2
ISEE=-ISEE
DO 410 IX=2, IIVM1
IV=IX
IF(ISEE.LT.0) IV=IIVP1-IX
IIVP1=IV+1
IIVM1=IV-1
JV1P1=JV1(IV)+1
JV2M1=JV2(IV)-1
ESTABLISH SPECIES EQUATION AT EACH GAS PHASE POINT
DO 420 JX=JV1P1, JV2M1
JV=JX
IF(ISEE.LT.0) JV=IIVP1-JX
JVPI=JV+1
JVM1=JV-1
I=(IV-1)*2+1
J=(JV-1)*2+1
FII=1.
FJI=1.
FJJ=1.
FKK=1.
COEFF=12.
NUMK1=20
IF(IV.EQ.2) GO TO 430
CONTINUE
IF(IV.EQ.IIVM1) GO TO 431
CONTINUE
IF(JV.EQ.2) GO TO 432
CONTINUE
IF(JV.EQ.JV2M1) GO TO 433
CONTINUE
IF(IV.LE.IV1. AND.JV.EQ.JV1P1) GO TO 434
CONTINUE
IF(IV.LE.IV1. AND.JV.EQ.JV2M1) GO TO 435
CONTINUE
IF(IV.GE.IV2. AND.JV.EQ.JV1P1) GO TO 438
CONTINUE
IF(IV.GE.IV2. AND.JV.EQ.JV2M1) GO TO 439
CONTINUE

404

C

```

991. CONTINUE
992. IF(K.EQ.2) GO TO 442
993. CONTINUE
994. DO 464 NV=1,NVENT
995. IVE=I(VVENT(NV))
996. JVE=J(VVENT(NV))
997. IF(CIV.EQ.IVE.AND.JV.EQ.JVE.AND.K.EQ.2.AND.VOLV.GT.0.)
998. #PHI(CIV,JV,I,L)=0.
999. CONTINUE
1000. CONTINUE
1001. GO TO 445
1002. COEFF=11.
1003. FII=0.450
1004. GO TO 450
1005. COEFF=11
1006. FII=0.451
1007. GO TO 451
1008. COEFF=11
1009. FJI=0.452
1010. GO TO 452
1011. COEFF=11.
1012. FJJ=0.453
1013. GO TO 453
1014. COEFF=10.
1015. FJI=0.
1016. GO TO 454
1017. COEFF=10.
1018. FJJ=0.
1019. GO TO 455
1020. COEFF=10.
1021. FJI=0.
1022. GO TO 456
1023. COEFF=10.
1024. FJI=0.
1025. GO TO 457
1026. COEFF=10.
1027. FJI=0.
1028. GO TO 458
1029. COEFF=10.
1030. FJI=0.
1031. GO TO 459
1032. COEFF=10.
1033. FJI=0.
1034. GO TO 460
1035. COEFF=10.
1036. FJI=0.
1037. GO TO 460
1038. COEFF=10.
1039. FJI=0.
1040. GO TO 460
1041. COEFF=10.
1042. FJI=0.
1043. COEFF=10.
1044. FJI=0.
1045. FJI=0.

```

```

1046. GO TO 461
1047. IF(KF.EQ.1.AND.IV.EQ.IF.AND.JV.EQ.JF) GO TO 462
1048. CDEFF=CDEFF-4
1049. FK1=0.
1050. GO TO 462
1051. CONTINUE
1052. CONTINUE
1053. CALCULATE DIMENSIONLESS SPECIES CONCENTRATION AT A POINT
1054. A1=A0*DIFFO(L)
1055. IF(L.EQ.2) A1=A0*DIFFO(12)
1056. FORMAT(5X,6(I2,1X),3(E10,3,1X))
1057. TCA=CAD(CIV,JV) +A1*(FI*PHI(IVP1,JV,K,L)+FI1*
1058. #PHI(CIVM1,JV,K,L)+FJJ*PHI(IV,JVPI,K,L)+FJI*PHI(IV,JVM1,K,L)
1059. #+FKK*PHI(IV,JV,KP1,L)*4. +4.*FK1*PHI(IV,JV,KM1,L))
1060. KCON=KM1
1061. IF(VOLV.LT.0.) KCON=KP1
1062. ICON=IVM1
1063. IF(VXC(I,J,K).LT.0.) ICON=IVP1
1064. JCON=JVM1
1065. IF(VYCI(J,K).LT.0.) JCON=JVP1
1066. IF(VOLV.LT.0.) AND.KFLAS.EQ.1) KCON=KM1
1067. TCA=TCA+A2*ABSCVX(CI,J,K))*PHI(CICON,JV,K,L)
1068. #+A3*ABSCVZ(CI,J,K))*PHI(CIV,JCON,K,L)
1069. #+A3*ABSCVZ(CI,J,K))*PHI(CIV,JV,KCON,L)
1070. PHIC(IV,JV,K,L)=TCA/(1.+A1*CDEFF+
1071. #A2*ABSCVX(CI,J,K))+A2*ABSCVZ(CI,J,K))+A3*ABSCVZ(CI,J,KCON))
1072. POSITIONAL RE-SET
1073. IF(CFII.EQ.0.) PHIC(IVM1,JV,K,L)=PHIC(IV,JV,K,L)
1074. IF(CFII.EQ.0.) PHIC(IVP1,JV,K,L)=PHIC(IV,JV,K,L)
1075. IF(CFJI.EQ.0.) PHIC(IV,JVM1,K,L)=PHIC(IV,JV,K,L)
1076. IF(CFJJ.EQ.0.) PHIC(IV,JVPI,K,L)=PHIC(IV,JV,K,L)
1077. IF(CFKI.EQ.0.) PHIC(IV,JV,KM1,L)=PHIC(IV,JV,K,L)
1078. IF(CFKK.EQ.0.) PHIC(IV,JV,KP1,L)=PHIC(IV,JV,K,L)
1079. CONTINUE
1080. CONTINUE
1081. CONTINUE
1082. CONTINUE
1083. CONTINUE
1084. DO 482 L=1,LEND
1085. IF(Z(L).LT.1.E-10)GO TO 482
1086. IF(L.EQ.18.AND.KFLAS.EQ.0) GO TO 482
1087. CALCULATE SPECIES CONCENTRATION FROM DIMENSIONLESS CONCENTRATION
1088. DO 482 K=1,KKM1
1089. DO 482 IV=1,IIV
1090. DO 482 JV=1,IJV
1091. IF(KF.EQ.1.AND.IV.EQ.IF.AND.JV.EQ.JF.AND.K.EQ.1)GO TO 482
1092. CAC(IV,JV,K,L)=CAC(IV,JV,KK,L)*(PHIC(IV,JV,K,1)+(PHI(IV,JV,K,2)-
1093. #PHI(IV,JV,K,1))*DR(L))
1094. CONTINUE
1095. C=P/(10.73*(TG(11,11,2)+460.))
1096. IF(KFLAS.NE.0) GO TO 522
1097. DO 520 K=1,KK
1098. DO 520 IV=1,IIV
1099. DO 520 JV=1,IJV
1100. SUM=0.

```

```

11101. DO 521 L=1,LEND
11102. DIFCL=EQ.18.AND.KFLAS.EQ.0) GO TO 521
11103. SUM=SUM+CACIV,JV,K,L)
11104. CONTINUE
11105. CACIV,JV,K,18)=C-SUM
11106. SUMNL=0
11107. GO TO 523
11108. PHIC(IF,JF,KF,1)=CACIF,JF,KF,1)/CA(IF,JREF,KK,1)
11109. PHIC(IF,JF,KF,2)=CACIF,JF,KF,12)/CA(IF,JREF,KK,12)
11110. CONTINUE
11111. C
11112. IF(CLTIME.LT.6)GO TO 584
11113. IF(CLCOMP.EQ.0)GO TO 584
11114. IXTIM=EXTIM+.0001
11115. IF(CLCOMP.EQ.IXTIM.OR.LCOMP.EQ.25) GO TO 590
11116. GO TO 584
11117. DO 561 LL=1,LEND
11118. IF(Z(LL).LT.1.E-10) GO TO 561
11119. WRITE(NH,562)XNAM1(LL),XNAM2(LL)
11120. FORMAT(5X,'COMPOSITION PROFILE FOR ',2A4)
11121. DO 563 IJK=1,2
11122. IF(IJK.EQ.1)WRITE(NW,564)
11123. FORMAT(5X,'MOLE FRACTION')
11124. IF(IJK.EQ.2)WRITE(NW,565)
11125. FORMAT(5X,'MASS FRACTION')
11126. DO 566 K=1,KK
11127. JSTAR=JV1(ISET)
11128. JEND=JV2(ISET)
11129. DO 567 J=JSTAR,JEND
11130. CTOT=0.
11131. DO 568 L=1,LEND
11132. ABC=1.
11133. IF(IJK.EQ.2) ABC=MW(L)
11134. CTOT=CTOT+CAC(ISET,J,K,L)*ABC
11135. ABC=1.
11136. IF(IJK.EQ.2) ABC=MW(LL)
11137. CX(J)=ABC*CAC(ISET,J,K,LL)/CTOT
11138. CONTINUE
11139. WRITE(NW,110)(CX(J),J=JSTAR,JEND)
11140. CONTINUE
11141. CONTINUE
11142. CONTINUE
11143. DO 412 IV=1,IIV
11144. JV1PI=JV1(IV)
11145. JV2MI=JV2(IV)
11146. DO 412 JV=JV1PI,JV2MI
11147. SUMNA=0.
11148. BT=TL-XI(1)
11149. CT=BT*(TL-XI(2))
11150. DO 555 L=1,LEND
11151. CALCULATE SPECIES FLUX AT EACH POINT ON LIQUID SURFACE
11152. IF(Z(L).LT.1.E-10) GO TO 555
11153. IF(L.EQ.18.AND.KFLAS.EQ.0) GO TO 555
11154. NA=-DIFFD(L)*CACIV,JV,KK,L)-CACIV,JV,KK,1.L)/(DELX)
11155.

```



```

1266. SKY=DEW*(TA+460.)
1267. QSOLD=0.
1268. QSOLW=0.
1269. QSOLW=0.
1270. IF(CLEAR.LT.0.) GO TO 610
1271. IF(EXTIM.LT.TDWN.OR.EXTIM.GT.TSET) GO TO 610
1272. CALCULATE SOLAR ANGLE
1273. W=-WS+15.*(EXTIM-TDWN)
1274. WSTOP=W+90.
1275. WGN=W-90.
1276. CW=COS(C3.14*W/180.)
1277. SW=SYN(C3.14*W/180.)
1278. COSO=SDEL*SPHI+CDEL*CPHI*CW
1279. IF(COSO.LT.0.) COSO=0.
1280. DO=3.14/2.
1281. DO=601 I=1,10
1282. DO=0-(COSO-COS(DO))/SIN(DO)
1283. TAUB=80
1284. IF(COSO.GT.01) TAUB=80+B1*EXP(-KSUN/COSO)
1285. ITAUD=.271-.2939*TAUB
1286. ITOT=CLEAR*(TAUB+TAUD)*IO
1287. CALCULATE TOTAL INCIDENT DIFFUSE RADIATION
1288. IO=IDI*ITOT*COSO
1289. CALCULATE TOTAL INCIDENT BEAM RADIATION
1290. IB=ITOT*COSO-ID
1291. CALCULATE TOTAL DOME INCIDENT SOLAR RADIATION
1292. QSOLD=ITOT*COSO
1293. CONTINUE
1294. C
1295. C
1296. C
1297. C
1298. C
1299. C
1300. C
1301. C
1302. C
1303. C
1304. C
1305. C
1306. C
1307. C
1308. C
1309. C
1310. C
1311. C
1312. C
1313. C
1314. C
1315. C
1316. C
1317. C
1318. C
1319. C
1320. C

```

```

1321. 604 CONTINUE
1322. C CALCULATE EXTERIOR TEMPERATURES 计算室外空气温度及辐射等效空气温度
1323. TDOO=TDOE(I)
1324. C1=TSKY**I4+(SLRCR**TDOO/DELTA+UW*(TA+460.))-QRADH+QSOLE*EWO)/(SIG*
1325. EWO)
1326. C2=(SLRCM/DELTA+UW)/(SIG*EWO)
1327. DO 631 I=1,10
1328. TDOE(I)=(C3.*TDOE(I)**I4+C1)/(4.*TWDE(I)**I3+C2)
1329. TDOO=TDOE(I)
1330. C1=TSKY**I4+(SLRCR**TDOO/DELTA+UW*(TA+460.))-QRADH+QSOLW*EWO)/(SIG*
1331. EWO)
1332. C2=(SLRCM/DELTA+UW)/(SIG*EWO)
1333. DO 632 I=1,10
1334. TDOE(I)=(C3.*TDOE(I)**I4+C1)/(4.*TDOM(I)**I3+C2)
1335. TDOO=TDOE(I)
1336. QW=QRADM-KG*(TGI,JPI,KAVE)-TG(I,JPO,KAVE))/DELX
1337. TWH(I)=-QW*SLKH+TDOM(I)
1338. QW=QRADM-KG*(TGI,J2MI,KAVE)-TG(I,J2MO,KAVE))/DELX
1339. TWE(I)=-QW*SLKW+TDOE(I)
1340. TALL GAS TEMPERATURES AT THE WALLS 计算室内空气温度及辐射等效空气温度
1341. DO 605 K=2,KK
1342. TG(I,J1PO,K)=TWIN(I)-460.
1343. TG(I,J2MO,K)=TWE(I)-460.
1344. TWA=TWA+TWE(I)+TWIN(I)
1345. CONTINUE
1346. TWA=TWA/(2.*II)
1347. TDOO=TDO
1348. IF(CLEAR.LT.0.)TDO=TA+460.
1349. IF(CLEAR.LT.0.)GO TO 608
1350. C1=TSKY**I4+(SLRCD*TDOO/DELTA+UD*(TA+460.))-QRAO+QSOLD*EDO)/(SIG*
1351. EDO)
1352. C2=(SLRCD/DELTA+UD)/(SIG*EDO)
1353. DO 633 I=1,10
1354. TDOE(I)=(C3.*TDOE(I)**I4+C1)/(4.*TDO**I3+C2)
1355. TDOO=TDOE(I)
1356. TDI=-QD*SLKO+TDO
1357. TL=(((-QRADL+SUNNL+TG(I,11,KK1)*KG/DELX)*FILMH+TBLK*KL)/(
1358. *FILMH*KG/DELX+KL)
1359. *XF=H/R
1360. C CALCULATE VIEW FACTORS
1361. F13=1.-.62*XF+.158*XF*(XF-1.)
1362. F31=F13
1363. F12=1.-F13
1364. F32=1.-F13
1365. F21=F32/(2.*XF)
1366. F23=F21
1367. C CALCULATE INTERNAL DOME, WALL AND LIQUID SURFACE RADIATION
1368. E1=SIG*TDO**I4
1369. E2=SIG*TWA**I4
1370. E3=SIG*(TL+460.)**I4
1371. C CALCULATE RADIOSITIES
1372. DO 615 I=1,10
1373. JD=(EDI**E1+(1.-EDI)*(F12**JL))/(EDI+(1.-EDI)*(F12+F13))
1374. JW=(EWI**E2+(1.-EWI)*(F21**JL))/(EWI+(1.-EWI)*(F21+F23))
1375. JL=(EL**E3+(1.-EL)*(F31**JW))/(EL+(1.-EL)*(F31+F32))

```

1376.
1377.
1378.
1379.
1380.
1381.
1382.
1383.
1384.
1385.
1386.
1387.
1388.
1389.
1390.
1391.
1392.
1393.
1394.
1395.
1396.
1397.
1398.
1399.
1400.
1401.
1402.
1403.
1404.
1405.
1406.
1407.
1408.
1409.
1410.
1411.
1412.
1413.
1414.
1415.
1416.
1417.
1418.
1419.
1420.
1421.
1422.
1423.
1424.
1425.
1426.
1427.
1428.
1429.
1430.

C 615 C CONTINUE
CALCULATE NET RADIATION FROM AN INTERIOR SURFACE

RADD=(J0-JH)*F12+(JD-JL)*F13
RADW=(JW-JD)*F21+(JH-JL)*F23
RADL=(JL-JD)*F31+(JL-JW)*F32
QRADD=ADD+RADF*(RADD-ADD)
QRADW=ADW+RADF*(RADW-ADW)
QRADL=ADL+RADF*(RADL-ADL)
ADD=QRADD
ADW=QRADW
ADL=QRADL

630 C CONTINUE
DD 625 I=1, II
J1M0=J1(I)
J2M0=J2(I)
DD 625 J=J1M0, J2M0
TG(I, J, I)=TDI-460.

625 TG(I, J, I)=TL
TG(I, J, KK)=T
IF(KFLAS.EQ.1)TG(IFLAS, JFLAS, KK)=T
IF(KFLAS.EQ.2)TG(IFLAS, JFLAS, 1)=T
IF(VOLV.LE.0.)GO TO 617

618 JVE=I
617 JVE=JVENT(I)
TG(I, J, I)=TA
C CONTINUE
J1PI=J1(I)+1
J2M1=J2(I)-1

606 DD 606 J=J1PI, J2M1
TG(I, J, I)=TDI-460.
TG(I, J, I)=T
IF(KFLAS.EQ.1)TG(IFLAS, JFLAS, 1)=T
IF(KFLAS.EQ.2)TG(IFLAS, JFLAS, KK)=T
A3=A0*4.*ALPHA
DD 612 KX=2, KKM1

C 613 K=KX
IF(VOLV.LT.0.) K=KK+1-KX
KPI=K+1
KM1=K-1
CALCULATE GAS PHASE TEMPERATURES
DD 613 I=1, II
DD 613 J=1, JJ
TG(I, J)=TG(I, J, K)
ISEE=-1
DD 616 ICONV=1, 2
ISEE=-ISEE
DD 611 IX=2, IIM1
I=IX

IF(ISEE.LT.0) I=II+1-IX
IPI=I+1
IIM1=I-1
J1PI=J1(I)+1
J2M1=J2(I)-1
DD 611 JX=J1PI, J2M1
J=JX

1486.
1487.
1488.

IF(VLE.LT.0.) VLE=XKVLE(1,1,LL)
RETURN
END

CARS LIBRARY



08309